Thesis/
Reports
Sadeh,
W. Z.

ESTIMATING THE POWER-LAW INDEX FOR WIND

Willy Z. Sadeh

Estimating the Power-Law Index for Wind

Willy Z. Sadeh, Yehuda Baron, and Douglas G. Fox

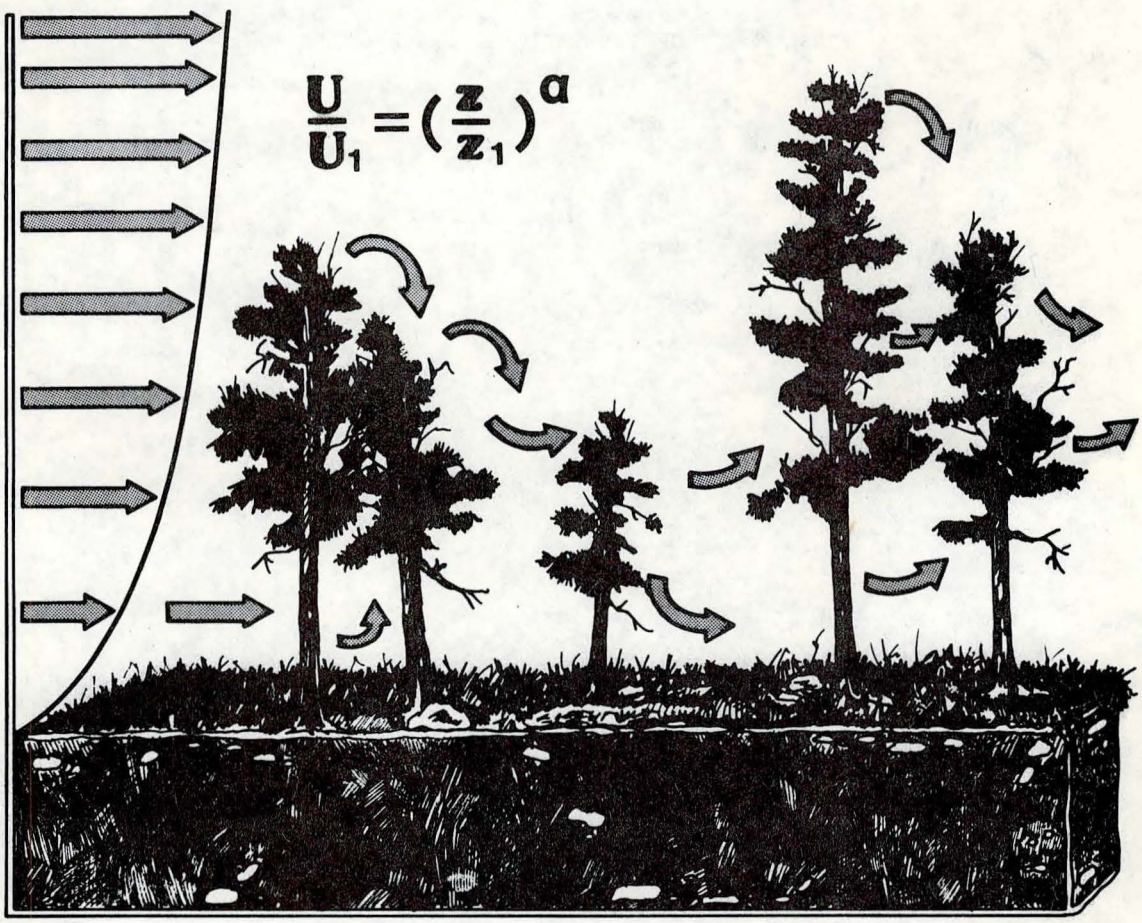

Rocky Mountain Forest and
Range Experiment Station
Forest Service
U.S. Department of Agriculture

LIBRARY COPY
ROCKY MT. FOREST & RANGE
EXPERIMENT STATION

ESTIMATING THE POWER-LAW INDEX FOR WIND

Willy Z. Sadeh,[1] Yehuda Baron,[2] and Douglas G. Fox[3]

FINAL REPORT OF COOPERATIVE RESEARCH AGREEMENT

16-934-CA

between the Rocky Mountain Forest and Range Experiment Station

and

Colorado State University

---

[1]Professor of Engineering and Fluid Mechanics, Dept. of Civil Engineering, Colorado State University.
[2]Research Assistant, Dept. of Civil Engineering, Colorado State University.
[3]Chief Meteorologist, USDA Forest Service, Rocky Mountain Forest and Range Experiment Station, Fort Collins, Colo.

ABSTRACT

The reliability of the power law in describing the wind shear above surface roughness under thermally neutral conditions is examined. A method for determining the power-law index, which consists of a universal empirical correlation between it and a roughness-wind interaction parameter, is advanced. The interaction parameter is expressed by the product of a surface-roughness structure index and a reference-wind Reynolds number. Procedures for approximating these two parameters, along with the reference wind and height of the power law, are introduced. The method was successfully tested using representative data in flow above very fine, fine, and high surface roughness.

TABLE OF CONTENTS

		Page
1.	INTRODUCTION	1
2.	LOGARITHMIC LAW	2
3.	POWER LAW	3
	3.1 Reference height	4
	3.2 Power-law index	6
4.	POWER-LAW PARAMETERS	9
	4.1 Standard reference scales	9
	4.2 Surface-roughness structure index	11
	4.3 Wind conditions	13
	4.4 Roughness-wind interaction parameter	14
5.	POWER-LAW INDEX ESTIMATION	14
	5.1 Power-law index range	14
	5.2 Method for power-law index estimation	15
	5.3 Wind-shear data examination	16
	5.4 Power-law index variation	20
	5.5 Correlation between power-law index and roughness-wind interaction parameter	22
6.	SUMMARY AND CONCLUSION	24
REFERENCES		26
APPENDIX I	DERIVATION OF EQUATION (3.2)	29
APPENDIX II	DERIVATION OF EQUATION (3.4)	29
APPENDIX III	PARAMETERS OF EQUATION (4.1)	30
APPENDIX IV	ESTIMATION OF PARAMETERS GIVEN IN TABLES 4, 5, 6, and 7	31
	IV.1 Very fine surface roughness - Table 5	31
	IV.2 Fine surface roughness - Table 6	32
	IV.3 High surface roughness - Table 7	34
	IV.4 Wind-shear data	37

ESTIMATING THE POWER-LAW INDEX FOR WIND

Willy Z. Sadeh, Yehuda Baron, and Douglas G. Fox

1. INTRODUCTION

Knowledge of the wind variation within the planetary boundary layer (or the atmospheric boundary layer) is essential for estimating the turbulent transport of mass, momentum, and energy and/or any other transport process of interest. The wind shear--i.e., the wind variation with height--in the atmospheric boundary layer is determined by the prevailing turbulent shear stresses, the pressure gradient, the density gradient, the temperature gradient, and the earth's rotation (Coriolis force). Generally, the turbulent shear stresses are much larger than the viscous stresses and, hence, the latter can usually be neglected [1,2,3]. Thermal effects can be further disregarded in the case of relatively strong winds. The turbulent shear stresses are produced by the wind interaction with the earth's surface roughness (i.e., by surface friction), and their upward diffusion is effected by the turbulent momentum flux. As the surface roughness is greater, coarser, and more nonuniform, the higher are the turbulent shear stresses and the upward transport of turbulent momentum. The effect of the surface roughness and, therefore, of the turbulent shear stresses decreases with increasing height due to the dissipation of turbulent energy. As the turbulent shear stresses become completely negligible, a height is reached where the wind is solely determined by a balance between the pressure gradient and the Coriolis force, i.e., the gradient wind or the geostrophic wind. This height, i.e., the geostrophic height, defines the thickness of the planetary boundary layer. Its depth varies from 500 to 1000 m (1600 to 3300 ft) depending upon the particular surface roughness, the density, and temperature gradients [4]. A geostrophic height of about 800 m (2600 ft) is generally assumed for a barotropic atmosphere and uniform surface roughness [5]. On the other hand, for an adiabatic or nearly adiabatic atmosphere and for both rural and/or urban terrains an average geostrophic height of about 600 m (2000 ft) is commonly advanced [6].

The effect of the surface roughness is primarily confined within the surface boundary layer, which is the lower layer of the atmospheric boundary layer. In this layer the influence of the Coriolis force can be disregarded in comparison with that of the surface roughness whenever the Rossby number is greater than about 10 [2]. The Rossby number Ro, which is the ratio of a characteristic wind velocity U_o (with respect to the rotating earth) to the product of a characteristic length L and the Coriolis parameter f (the earth's angular velocity), i.e., $Ro = U_o/Lf$, accounts for the earth's rotation. Within the small-scale range of atmospheric motion that extends over a horizontal fetch up to about 16 km (10 miles) [2], the condition of a Rossby number of 10 or higher is generally met [depending, however, upon the magnitude of characteristic wind]. The pressure gradient is then simply treated as a constant driving force [4]. As a result, the turbulent shear stress is the main factor determining the wind shear in the surface boundary layer within the small-scale range of atmospheric motion under thermally neutral conditions.

The depth of the surface boundary layer is usually estimated assuming that the turbulent shear stress is either approximately constant [4,6,7; to mention only a few] or changes with height within a certain imposed range [1,8]. Currently, there is no consensus about the acceptable degree of turbulent shear stress variation with the depth of the surface boundary layer. Estimates of the surface boundary-layer depth varying from a minimum of 8 to 16 m (26 to 52 ft) [1] up to a maximum of about 200 m (650 ft) [8] have been proposed, depending upon the magnitude of the shear stresses at the surface and on its prescribed variation with height. For instance, a 5% maximum change in the shear stress with height is recommended in Ref. 1 whereas a variation up to 20% (four times higher) is suggested in Ref. 8. A depth of 50 to 100 m (160 to 330 ft) is, on the other hand, advanced in Ref. 4 without the variation of the shear stress with height being explicitly specified. For adiabatic or nearly adiabatic conditions, an average depth of about 100 m (330 ft) is introduced in Ref. 6 based on a review of field data.

Any change in the terrain roughness induces the development of an internal boundary layer within the lower layer of the surface boundary layer [9,10,11,12]. This layer results from the flow adjustment to the new underlying surface roughness. Its downwind rate of growth depends upon the specific terrain roughness and the prevailing upward diffusion of the turbulent shear stresses under thermally neutral conditions. The internal boundary layer is, consequently, characterized by a continuous variation of the turbulent shear stress from the surface to its outer edge [11,12]. Essentially, the latter separates the airflow affected by the new surface roughness from that above it which has not yet been altered. It is customary to define the thickness of the internal boundary layer as the height where the local turbulent shear stress is equal

to its counterpart in the undisturbed surface boundary layer at the leading edge of the new surface roughness [12]. The complex dependence of the wind shear within the internal boundary layer and, generally, within the surface boundary layer on the turbulent shear stress variation is not yet amenable to a satisfactory theoretical treatment. As a result, the wind shear in these layers is currently described by either a semi-empirical or an empirical method which is represented by the logarithmic law and the power law, respectively.

The underlying assumptions, properties, and current applications of both the logarithmic law and the power law under thermally neutral conditions were examined in view of their widespread use in describing the wind shear in the surface and/or internal boundary layers. To start with, a scrutiny of the logarithmic law was conducted in order to point out the drawbacks associated with determining its universal constant and its similarity scales, and the restriction imposed by its basic underlying assumption of a constant turbulent shear-stress layer. An examination of the power law was next performed for the sake of outlining its simplicity, expediency, and operational practicability in engineering applications. In order to identify the problems related to the use of the power law, a survey of the main methods employed to specify its two reference scales and to determine its index was carried out. Emphasis was placed on examining how the power-law index is commonly estimated since it indicates the effect of the surface roughness and, hence, of turbulence upon the wind shear. Consequently, the dependence of the power-law index upon the wind conditions and the surface roughness was reviewed. The ultimate objective of this work was to advance an empirical method for determining the power-law index over its entire range in terms of both the surface roughness and the wind conditions. To this end, a correlation relating the power-law index to suitable characteristic and readily measurable parameters of the surface roughness and the wind shear was sought.

2. LOGARITHMIC LAW

The wind variation is expressed in the semi-empirical method by the universal logarithmic law (or the log law) that was initially advanced by Prandtl to describe the streamwise mean velocity in a fully-developed turbulent boundary layer on a flat plate for steady flow of an incompressible fluid [4,13,14]. Essentially, the log law represents a similarity solution of the equations of motion for the streamwise mean velocity under thermally neutral conditions and under the customary assumption of: (1) zero transverse and vertical mean velocities; (2) zero streamwise pressure gradient, i.e., constant streamwise pressure; and (3) neglect of the Coriolis force. Then the universal log law was obtained based on the mixing-length theory under the far-reaching assumption of constant turbulent shear stress throughout the turbulent boundary layer. The usual form of the log law used to describe the wind shear $U(z)$ is [4]

$$U/U_* = (1/\kappa)\ln(z/z_0) , \qquad (2.1)$$

in which z denotes the vertical distance measured from the surface and κ stands for the so-called von Kármán universal constant. This universal constant is a dimensionless coefficient of proportionality relating the mixing length to the distance from the wall whose value is to be deduced from experiment. In the foregoing equation, the two similarity parameters are the friction velocity U_* and the roughness length z_0. The friction velocity $U_* = (\tau_0/\rho)^{\frac{1}{2}}$, where τ_0 is the turbulent shear stress at the wall (i.e., at $z = 0$) and ρ the density of the air in consistent units. According to the condition of constant turbulent shear stress throughout the turbulent boundary layer, the friction velocity is invariant with height. The roughness length z_0, which is the other similarity parameter, characterizes the surface roughness without, however, being equal to the physical height of the roughness elements. It is a constant of integration and, therefore, the log law applies only for $z \geq z_0$.

The log law in its original version, given by the foregoing equation, is restricted to turbulent flow over surfaces that are either bare or covered with fine roughness not exceeding several centimeters in height. In order to extend the log law to turbulent flow over relatively high roughness, such as tall vegetation or forest canopies, a purely empirical modification of the height, limited initially to roughness elements generally uniform in their distribution and height, was advanced [15,16]. This modified log law is given by [4],

$$U/U_* = (1/\kappa)\ln[(z - d)/z_0] , \qquad (2.2)$$

where the correction for the vertical coordinate is represented by the zero-plane displacement d. The latter is simply an adjustment of the vertical datum level so that all the turbulent exchange processes are considered to transpire above it. As a result, the modified log law holds solely for $z \geq z_0 + d$. It is apparent that the roughness length and the zero-plane displacement are interdependent since the log law was obtained by integrating a first-order differential equation. They are nevertheless considered as being two independent arbitrary constants usually estimated from the best fit curve to the measured wind shear [17]. One then can view the zero-plane displacement as an additional third similarity parameter of solely empirical nature characteristic to the particular high surface roughness. It is noteworthy to point out that no exact definition of high roughness has yet been offered. Roughness of a height exceeding 10% of the boundary-layer depth is generally viewed as high roughness [18]. In practice, the zero-plane displacement is introduced whenever the original log law (Eq. (2.1)) fails to reasonably describe the measured wind distribution.

In using the log law or its modified form three or four parameters are to be determined, viz., (1) the von Kármán universal constant κ; (2) the friction velocity U_*; (3) the roughness length z_0; and (4) the zero-plane displacement d (when the modified log law is employed). The last three parameters are essentially local similarity scales since they can vary in the streamwise direction. Generally, the von Kármán universal constant κ is assumed equal to 0.4 based on an extensive experimental study of fully developed turbulent flow through a pipe with smooth wall and a variety of fine surface roughness [19]. On the other hand, von Kármán found, based on other experimental results, that the value of this constant lies between 0.37 to 0.38 [13]. Estimates of this so-called universal constant varying from 0.29 to about 0.62 have been reported, depending upon the particular analysis of the wind data [20,21,22,23]. Even a startlingly small value of 0.22 for this constant was obtained in flow over high roughness in a wind tunnel [12]. A value of about 0.35 for the von Kármán constant was further deduced from its relationship to the Kolmogorov constant when the latter is 0.55 [21]. At the present time, it is customary to accept the initial value of 0.4 for the von Kármán constant despite the reported significant scattering in its magnitude.

The friction velocity U_* can basically be determined provided that the turbulent shear stress at the wall is known. Measurement of the shear stress τ_0 at the earth's surface is generally exceedingly difficult and even unfeasible in many instances because of the prevalent surface roughness, e.g., forest canopy, urban roughness. The friction velocity is consequently evaluated in practice from the measured velocity distribution if one accepts beforehand the familiar condition of its local invariance within the depth of the surface boundary layer or within a significant portion of it. This condition of locally constant shear stress is, in fact, the feeblest trait of the log law with regard to its use in describing the wind shear. The validity of this restrictive assumption is particularly questionable in the internal boundary layer in flow above high roughness and/or over changing surface roughness. Wind-tunnel and field surveys in flow above both fine and relatively high roughness clearly reveal that the turbulent shear stress and, hence, the friction velocity vary within the depth of the internal boundary layer [10,12,18,24,25]. A linear variation of the friction velocity with height, which was found to be in reasonable agreement with some field observations, was further proposed [11]. Currently, the condition of either invariant or constant change of the friction velocity with height [1,8] is considered acceptable in utilizing the log law, notwithstanding the apparent contradictory evidence.

The length similarity parameters of the log law and of its modified version--viz., the roughness length z_0 and the zero-plane displacement d--are intrinsically unmeasurable. They are determined by fitting the log law or its modified version to the measured wind shear. Empirical relationships for the roughness length z_0 have further been proposed for particular flow situations [26]. The complex dependence of these two length similarity parameters upon the height of the roughness elements is as yet not known. In wind-tunnel flow above high roughness it was found that the roughness length changes with depth when its local constancy was checked according to the modified log law [18]. It is important to stress that physically erroneous negative values for the zero-plane displacement d can often be obtained when it is estimated simultaneously with the other two similarity parameters (i.e., friction velocity U_* and roughness length z_0) by fitting the modified log law to given velocity data [12]. In order to overcome this difficulty, it is customary to approximate the zero-plane displacement d by the height of the roughness h provided that it is uniform, i.e., $d \cong h$ [12,27].

Both the log law and/or the modified log law are used to describe both atmospheric and/or wind-tunnel velocity data in spite of their inherent limitations. These two laws are employed even under a wide range of stability conditions since they supply a reasonable first-order approximation in many instances. This, however, should not lead to ignoring that the basic underlying condition of constant shear-stress layer is not met in numerous flows and, in particular, in the internal boundary layer above high roughness. One must furthermore bear in mind that the roughness length is not always a local constant and that the value of the von Kármán constant is not necessarily 0.4. It is thus imperative to pay close attention to each flow situation prior to applying the log law or the modified log law. This is of paramount importance with regard to describing the velocity distribution in the internal boundary layer above high roughness in the light of the significant variation of the turbulent shear stress within its depth.

3. POWER LAW

In the empirical approach the wind variation with height (i.e., the wind shear) is represented by a simple power-law profile, which was initially proposed almost a century ago [28,29]. The power law in its present form was introduced as a purely empirical similar velocity-distribution law for the mean velocity variation in a fully developed turbulent flow through a pipe and/or in a turbulent boundary on a flat plate [14]. It is widely used in describing the wind shear in the atmospheric surface and internal boundary layers in view of its expediency in engineering applications and in meteorological work [4,6,30, 31,32]. The power law is employed under conditions identical to those for the log law except for the restriction of constant shear stress throughout the boundary layer. In fact, the removal of the latter constraint makes the power law convenient to express the wind shear. In addition, the power law is often used to approximate the wind shear in the presence of a temperature gradient [4,30].

The general form of the power law for the wind shear U(z) is [4]

$$U/U_1 = (z/z_1)^{\alpha} , \qquad (3.1)$$

where z is the height measured from the surface, U_1 designates the reference wind at a reference height z_1, and α stands for the power-law index (or exponent). It is evident that the reference wind and height are the empirical similarity scales of the power law. Selection of the reference height z_1 and, necessarily, of its corresponding reference wind U_1 is presently quite arbitrary. Reference heights ranging from the geostrophic height down to the standard 10 m (30 ft) height above the surface have been used in attempting to account in each case for the specific surface roughness [6]. The depth of the internal boundary layer is, in all likelihood, a most attractive choice for the reference height considering that both the wind shear and the shear stress undergo their most significant variation within this layer. However, no clear criterion for the selection of the reference height and/or wind has thus far been advanced.

The effect of turbulence induced by the surface roughness upon the wind shear is represented in the power law by its index, whose value is smaller than unity and larger than zero. In addition, the value of the index depends upon the temperature gradient [4]. This third parameter of the power law is approximated by simply fitting the measured wind-shear data to the power law once the reference scales are established. The estimation of the power-law index is consequently affected by the choice of the similarity scales for a given surface roughness. Additionally, it was found in flow through a pipe that the power-law index depends slightly upon the flow Reynolds number (based on mean velocity and pipe diameter). To date, coarse estimates of the power-law index were proposed based on correlating measured wind shear with some gross characteristics of the surface roughness, using the geostrophic height and corresponding wind as the similarity scales [32]. The suggested representative values for the power-law index are: (1) 0.16 for flat open country; (2) 0.28 for wooded country and city suburbs; and (3) 0.40 for city-like type of roughness. However, extremely large discrepancies in the value of the power-law index are consistently found for almost any kind of surface roughness [6,33]. The reason for this is the lack of even a reasonable empirical model for the power-law index.

It is, however, apparent that the power law offers by and large a more dependable description of the wind shear than the log law. The higher reliability of the power law stems from the exclusion of constant shear-stress layer condition. Additional appealing features of the power law are its remarkable simplicity and operational practicability. It is therefore desirable to probe the use of the power law in the internal boundary layer because of the large gradients in the wind shear and shear stress that generally occur throughout this lowest layer of the surface boundary layer. Proper use of the power law depends upon the adequate selection of its similarity scales (z_1 and U_1) and, in particular, on the estimation of its index (α). In practice, the reference scales are first established and then the power-law index is approximated by means of the best fit curve to the wind data, as previously mentioned. It is evident that the two reference scales are related since the selection of either one specifies uniquely the other. The customary approach is first to determine the reference height.

3.1 Reference Height

To start with, the overall resemblance of the atmospheric boundary layer to an ordinary turbulent boundary layer on a smooth and/or rough flat plate suggests the selection of the geostrophic height as the reference height of the power law. The geostrophic height (the gradient height or level) depends upon the decay of the turbulence with the depth and the prevailing vertical temperature gradient. As a result of the former, the geostrophic height is affected by the surface roughness, which is the agent responsible for the production of turbulence. Determination of the geostrophic height is ambiguous since one cannot specify exactly the thickness of a boundary layer. Numerous methods for estimating the geostrophic height have consequently been advanced, but thus far all of them are restricted in their applicability. The difficulties associated with the approximation of the geostrophic height are best revealed by the extensive analysis of the 1953 O'Neill data reported in Ref. 34. Fourteen different methods are reviewed in this analysis and, generally, their agreement with the O'Neill observations is relatively limited. The most common approach at the present time is to estimate the geostrophic height as the level where the wind reaches its first maximum value, i.e., the level where the gradient wind is first attained [31]. In using this gradient-wind method one can obtain an average geostrophic height that accounts for the surface roughness and for the diurnal and even seasonal variation of the temperature gradient with depth.

In order to determine the geostrophic height by means of the gradient-wind method, it is necessary to measure the wind shear up to the height of its first maximum. Acquisition of such wind data is unfeasible in many situations due to the facilities required and economic constraints. Then the geostrophic height is estimated by extrapolating the power law up to the level of the gradient wind subsequent to fitting it to the available wind-shear data. This extrapolation procedure inherently leads to a gross approximation for the geostrophic height and, consequently, to wide disparities in its level. Several representative values for the geostrophic height above a variety of surface roughnesses are summarized in Table 1 below for the sake of illustrating the scattering in its proposed depth. These geostrophic heights were deduced: (1)

TABLE 1. REPRESENTATIVE VALUES OF THE GEOSTROPHIC HEIGHT

Approximation Procedure	Source	Ref.	Surface Roughness	Geostrophic Height (m)
Measurement	Hanna	34	Open country	450-700
	Thuillier & Lappe	35	Open country (small orchards)	300-360
Extrapolation	Sherlock	36	Open country	300
	Shellard	37	Open country	300-400
			City	
Extrapolation and seasonal averaging	Davenport	31	City	520
Averaging (with respect to surface roughness)	Davenport	31	Rough wooded country	400
	Davenport	33	City	425
	Counihan	6	Rural & urban country	600

based on measured wind-shear variation with height; (2) by the extrapolation procedure; and (3) by averaging with respect to the surface roughness. All of them were obtained under neutral and/or near neutral atmospheric conditions.

The general trend indicated by the results given in Table 1 is the increase in the geostrophic height with increasing height of the surface roughness. Geostrophic heights varying from 300 to 400 m (1000 to 1300 ft) are advanced for open-country roughness [35,36,37]. On the other hand, the O'Neill data, which were obtained over flat open country, indicate a geostrophic height between 450 and 700 m (1500 and 2300 ft), and depending upon the stability conditions [34]. An average geostrophic height of about 400 m (1300 ft) is proposed for rough wooded country [31]. In flow above a city, geostrophic heights from 300 to 520 m (1000 to 1700 ft) are recommended [31,33,37,38]. The lack of a consistent and systematic correlation between the height of the surface roughness and the geostrophic height is apparent.

The extent to which the height of the surface roughness affects the geostrophic height depends essentially upon the level of the turbulence produced by the very same surface roughness and the subsequent dissipation of this turbulence with height. In addition, the balance between the production and dissipation of the turbulence is influenced by the strength of the wind shear within the layer immediately above the surface roughness--i.e., within the internal boundary layer--and the stability conditions. Taller surface roughness promotes production of higher levels of turbulence, and then one can expect that its dissipation would transpire over a deeper range under moderate wind shear and neutral conditions. In other words, a higher geostrophic height is expected with increasing height of the surface roughness. The balance between the production and dissipation of turbulence with height is yet to be adequately modeled. Thus far it was suggested that the geostrophic height (or gradient level) grows relatively slowly with increasing height of the surface roughness [39]. This proposition is apparently in conflict with field results (see Table 1), which indicate a maximum augmentation in the geostrophic height of about 73%--viz., from 300 to 520 m--as the surface roughness changes from open country to city.

It is further interesting to note that a geostrophic height of roughly same depth for both high roughness and open country has been deduced in many field studies. An identical geostrophic height of about 300 to 400 m (1000 to 1300 ft) is, for instance, reported in Ref. 37 (see Table 1) in flow above both a city and open country. Similarly, an average geostrophic height of roughly 600 m (2000 ft) is proposed in Ref. 6 (see Table 1) for both rural and urban roughness under almost neutral conditions. The realization of a geostrophic height of about same depth above high surface roughness and open country is due, in all likelihood, to the presence of strong wind conditions in a shallow layer above the top of the high roughness. Such evidence is reported in Ref. 37. Hence, one can conjecture that the occurrence of a stronger wind shear within the internal boundary layer above high surface roughness fosters the dissipation of turbulence to a larger extent than its production. The role played by a strong wind shear in lowering the geostrophic height above high surface roughness is yet to be investigated. It is thus apparent that one cannot assume a priori a certain geostrophic height for a given surface roughness without measuring the wind-shear variation with depth. The geostrophic heights outlined in Table 1 are to be viewed as simply being

indicative of their overall order of magnitude for each particular surface roughness.

The use of the power law in describing the wind shear should not hinge on any unique reference height due to its purely empirical nature. Undoubtedly, the geostrophic height is an attractive choice since it represents the thickness of the atmospheric boundary layer. Nothing is, however, sacred with regard to its selection as the reference height. Adoption of the geostrophic height as the reference height is, moreover, almost precluded in many flow and surface roughness conditions because of the significant difficulties in obtaining a reliable estimate for it. The major drawback to employing the geostrophic height is the intrinsic difficulty associated with its direct measurement. It is, therefore, desirable to select a convenient reference height near the surface that permits one to readily measure the reference wind shear. Attempts to express the power law in terms of the standard 10 m (30 ft) height and wind have consequently been undertaken [32,40,41]. This arbitrary selection of the two similarity scales for the power law is unfortunately restricted to open-country roughness.

The gradual decay with height of the turbulence produced by the surface roughness is the prime factor affecting the selection of the reference height under neutral and/or near neutral conditions. Production of turbulence by the surface roughness is concentrated within its internal boundary layer. Most of this turbulence dissipates in the very same layer. Generally, the dissipation beyond the height of the internal boundary layer is quite small. This is particularly true in flow above relatively high surface roughness, such as wooded country and urban area, in the presence of a strong wind. It is therefore reasonable to choose the depth of the internal boundary layer as the reference height of the power law. Such a similarity length scale would better reflect the effect of the surface roughness upon both the production and dissipation of turbulence. Further exploration of this approach is undoubtedly warranted. It is further important to point out that the value of the power-law index depends upon the choice of the reference height, the corresponding reference wind, and the fitting of the power law to the observed wind shear.

3.2 Power-Law Index

Specification of the reference scales of the power law for given wind-shear data necessarily determines a unique estimate for the power-law index through the best fit curve. The power-law index accounts then for the wind-shear variation, the production of turbulence by the surface roughness, and the dissipation of turbulence with depth in a similar manner as the reference height and wind. In the light of the overall identical dependence of all the three parameters of the power law upon the wind shear and turbulence characteristics, the feasibility of empirically correlating the power-law index α with the reference level wind was explored. The rationale for such a correlation is that the reference wind and its corresponding height (or level) reflect the prevailing wind shear and, particularly, the turbulence characteristics within the layer of interest. As a matter of fact, the reference level wind changes depending upon the strength of the wind shear and the prevalent turbulence and, therefore, one can view it as an indicative parameter insofar as the power-law index is concerned.

Typical attempts to correlate the power-law index α with a reference level wind can be found in Refs. 41 and 42. In both cases the wind at 10 m height U_{10} is suggested as the reference wind. The dependence of the power-law index α on the 10 m height average reference wind (5 min average) is given in Ref. 41 in a simple tabular form for the latter ranging from 4.5 to 31.3 m/s (10 to 70 mph). Within this range of relatively strong 10 m height reference wind, the power-law index increases from 0.19 to 0.31, i.e., by 63%. Inspection of the data reported in Ref. 41 reveals that this correlation can be expressed by the linear relationship (see Appendix I)

$$\alpha = 0.0046U_{10} + 0.17 \quad , \qquad (3.2)$$

in which U_{10} is the value of the average reference wind measured in meters per second. This linear increase of the power-law index with increasing 10 m height reference wind is portrayed in Fig. 3.1.

Examination of field wind data at 19 different sites of a wide variety of surface roughness, which are compiled in Ref. 31, indicates a similar trend for the power-law index with increasing wind strength. These field wind data were collected above a height of 10 m in strong winds under adiabatic and/or nearly adiabatic conditions, and their power-law description is based on the 10 m height reference wind. Analysis of wind data measured at Brookhaven National Laboratory under weak superadiabatic conditions reveals also that the value of the power-law index increases with increasing wind speed [30]. No attempts to express the increase in the value

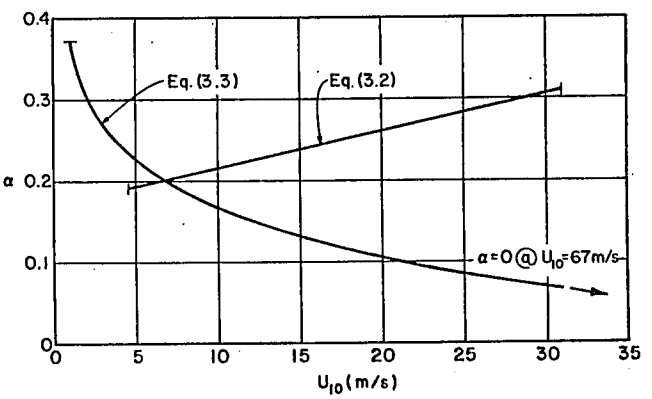

Figure 3.1--Variation of the power-law index with increasing 10 m height reference wind.

of the power-law index in terms of the 10 m height reference wind or other reference wind were advanced in these two cases [30,31].

It is important to point out that increasing 10 m height reference wind indicates the occurrence of stronger wind conditions and higher turbulence level in the layer immediately above the surface roughness, i.e., within the internal boundary layer. These stronger wind conditions promote, in turn, the dissipation of turbulence within a thinner layer, as previously mentioned. Thus, the increase in the value of the power-law index with stronger 10 m height reference wind reflects these turbulent conditions. A flatter wind shear variation with height is then obtained, according to the power law, since the geostrophic height is lowered.

The dependence of the power-law index upon the 10 m height reference wind proposed in Ref. 42 is diametrically opposite in its nature to that suggested in Ref. 41. A continuous decrease in the value of the power-law index α with increasing 10 m height average reference wind (1 min average) described by the following empirical logarithmic relationship

$$\alpha = 0.37 - 0.0881 \ell n U_{10} \quad , \qquad (3.3)$$

is submitted in Ref. 42. In this expression U_{10} stands also for the value of the average reference wind measured in meters per second. The two constants in the foregoing relation are viewed by their proponents as being universal notwithstanding that they were obtained assuming a Weibull distribution [43] for the wind speed and using wind-shear data from only four different sites. A uniform decrease in the power-law index from 0.37 to zero as U_{10} increases from 1 to a very high speed of 67 m/s (2.24 to 150 mph) is indicated by Eq. (3.3). It is apparent that the use of this equation is restricted to a certain reference-wind speed range, but such a suggestion was not advanced in Ref. 42.

The variation of the power-law index with increasing 10 m height reference wind according to Eq. (3.3) is displayed in Fig. 3.1 along with its linear increase advocated by Eq. (3.2) for the sake of pointing out their opposing trends. One can easily note that the relative difference in the estimate for the power-law index offered by these two empirical relations becomes greater with increasing reference wind. For instance, their relative difference (based on α given by Eq. (3.2)) increases from 22% to 59% as the reference wind increases from 10 to 20 m/s (22.40 to 44.74 mph). In view of the empirical nature of these two relationships, one cannot readily assess which offers a better approximation of the power-law index. In fact, the validity of both relations is disputable since they were obtained based solely on a reference level wind. Their main limitations are, in all likelihood, (1) not accounting for the surface roughness and (2) not taking into consideration a particular reference level wind. The latter is undoubtedly affected by the surface roughness, but thus far their interdependence is yet to be explicitly outlined. Evidence with regard to the role of the surface roughness in affecting, for instance, the so-called two universal constants in Eq. (3.3) can be found in Ref. 44. In attempting to apply Eq. (3.3) to wind data at two sites of slightly different surface roughness, drastically different values of these two constants were found [44]. The first coefficient varied by ±22% while the change in the second coefficient was from +2% to about +93%. It is thus apparent that it is imperative to consider the effect of the surface roughness on the power-law index in addition to the effect of the reference wind.

Numerous efforts to identify the dependence of the power-law index upon the surface roughness have been undertaken. These endeavors are best represented by the procedures proposed in Refs. 31, 32, and 6 published in 1960, 1963, and 1975, respectively. In attempting to ascertain the effect of the surface roughness, it is necessary to represent it in terms of a single characteristic parameter. The roughness length z_0, which is one of the similarity parameters of the log law, is commonly used to describe the surface roughness. It is an empirical parameter that cannot be physically measured and that is generally deduced by fitting the wind-shear data to the log law, as previously mentioned. The roughness length is consequently beset by the basic constraints of the log law. Nevertheless, the roughness length is widely employed despite its inherent limitation since it is a convenient parameter with regard to indicating the height of the roughness. As the latter is higher and rougher, the roughness length is greater.

An interesting attempt to express the dependence of the power-law index on the surface roughness by means of the roughness length can be found in Refs. 31 and 32. Based on wind-shear data obtained for strong winds and under neutral conditions at more than 19 sites ranging in their surface roughness from open sea to a large city center [31], the variation of the power-law index with increasing roughness length was represented in terms of a nomogram in Ref. 32. In each case, the roughness length was deduced from the wind-shear data near the ground by means of the log law. The nomogram was constructed by: (1) considering the main four classes of surface roughness, viz., open sea (or smooth), flat open country (or moderately rough), woodland forest (or rough), and urban area (or very rough); (2) specifying a roughness-length range for each class of terrain; and (3) using single average values of the power-law index α for the last three classes of surface roughness, viz., α = 0.16, 0.28, and 0.40 for flat open country, woodland forest, and urban area, respectively.

Examination of the variation of the power-law index with increasing roughness length shown in the nomogram given in Ref. 32 reveals that it can be approximated by the relationship (see Appendix II)

$$\alpha = 0.125 \ell og z_0 + 0.0004/z_0 + 0.336 \quad , \qquad (3.4)$$

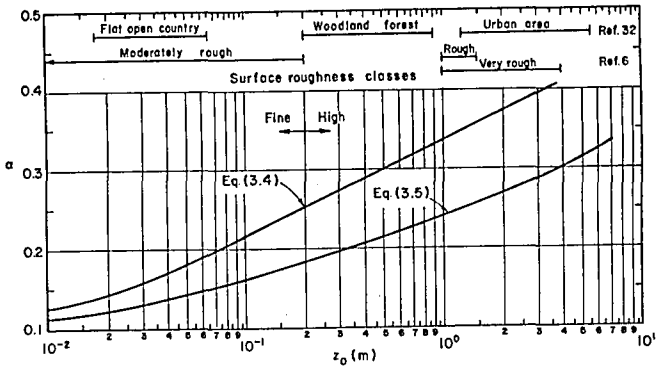

Figure 3.2.--Variation of the power-law index with increasing roughness length and corresponding surface roughness classes.

over a roughness-length range z_0 = 0.01 to 5.5 m (0.03 to 18 ft), i.e., flat open country (or moderately rough) to urban area (or very rough). In the foregoing equation z_0 designates the value of the roughness length given in meters. The continuous increase in the power-law index with augmenting roughness length described by Eq. (3.4) is displayed in Fig. 3.2. Greater roughness length signifies higher roughness, which, in turn, fosters production of turbulence. Consequently, one can attribute the increase in the power-law index to the occurrence of higher level of turbulence. It is interesting to point out that a similar variation in the power-law index is suggested by Eq. (3.2) for stronger 10 m height reference wind.

Another typical effort to identify the dependence of the power-law index α on the roughness length z_0 is outlined in Ref. 6. This attempt is quite similar to that introduced in Ref. 32. Wind-shear data from 70 different sites encompassing all four main types of surface roughness were used in this undertaking. Adiabatic conditions were assumed in considering these wind-shear data even if they were not completely established. The roughness length was then computed by means of the log law and/or the modified log law, depending upon the surface roughness, using wind-shear data up to a height of 100 m (328 ft). A power-law index was estimated in each case from a single pair of wind-shear data at two consecutive heights, implying a two-point piecewise wind-shear linear change. Subsequently, a single mean power-law index was computed for each wind-shear profile by averaging over all the two-point indexes. The increase in the mean power-law indexes with increasing roughness length was finally approximated by the following relationship:

$$\alpha = 0.096 \log z_0 + 0.016(\log z_0)^2 + 0.24 \quad , \quad (3.5)$$

for $0.001 \leq z_0(m) \leq 5$ and despite a significant scattering in the data. In this relationship z_0 simply denotes the value of the roughness length given in meters. It is interesting to note that the foregoing relationship was considered by its own proponent as representing, to some extent, a subjective interpretation of the data in view of the two-point piecewise procedure used to approximate the mean power-law indexes.

The variation of the power-law index according to Eq. (3.5) together with that described by Eq. (3.4) are portrayed in Fig. 3.2 for the sake of simultaneously stressing their qualitative similarity and quantitative difference. Essentially, these two empirical relationships differ only in the particular numerical value of the power-law index for a given roughness length. The approximation offered by Eq. (3.4) is consistently larger than that advanced by Eq. (3.5), and the difference between them becomes greater with increasing surface roughness. For example, at roughness lengths of 0.02 and 2 m (0.066 and 6.6 ft; flat open country and urban area), the estimates for the power-law index according to Eq. (3.4) are 17% and 38% greater than those set forth by Eq. (3.5). This continuously increasing discrepancy can, in all likelihood, be attributed to the different procedures used to relate the power-law index to the surface roughness.

Particularly revealing are the significant disparities in the proposed ranges of the roughness length for the four main classes of surface roughness. In order to point out these differences, the proposed ranges of the roughness length are summarized in Table 2 below. These roughness-length ranges, except the one for smooth terrain (or open sea), are illustrated in Fig. 3.2. The lack of agreement in the suggested ranges of roughness length is readily discerned. For instance, for rough terrain, which includes woods, a roughness length varying from 1 to 1.5 m (3.3 to 4.9 ft) is proposed in Ref. 6, while for similar woodland forest the range recommended in Ref. 32 is from 0.2 to 0.9 m (0.66 to 3 ft). Another area of concern is the lack of any suggestion of roughness lengths for the transition terrain between two main categories of surface roughness, as clearly seen in Fig. 3.2. No further explanation is offered in Ref. 6 for the overlapping in the roughness length for rough and very rough terrains shown in Fig. 3.2. In the light of the uncertainty associated with determining the roughness length and, moreover, in view of its derivation by means of the log law, one can question whether it is to be considered as the characteristic parameter of the surface roughness. The need for exploring the possibility of introducing a more reliable and directly measurable parameter to characterize the surface roughness is apparent.

The approximation advanced by either Eq. (3.4) or (3.5) is to be viewed in practice as being only indicative of the change in the power-law index with increasing roughness length. The use of either approximation is basically contingent upon knowing beforehand the roughness length. This stringent requirement cannot be met since the roughness length is derived by assuming a logarithmic wind-shear variation near the ground. The other possibility is to arbitrarily surmise a roughness length for each particular terrain within the ranges advanced for each class of surface roughness. But then it is necessary

TABLE 2. ROUGHNESS LENGTH RANGES

Surface Roughness	Roughness Length z_0 (m)	
	Davenport [32]	Counihan [6]
Open sea Smooth (ice, mud, snow, sea)	0.00024-0.0034	0.00001-0.02
Flat open country Moderately rough (short grass, grass, crops, rural)	0.0175-0.065	0.001-0.20
Woodland forest Rough (rural, woods, suburbs)	0.2-0.9	1-1.5
Urban area Very rough (urban)	1.25-5.5	1-4

to make a choice among the ranges recommended in Refs. 6 and 32. Thus far, no objective criterion for making such a selection was offered. Discretionary advancing of the roughness length leads to a large uncertainty in the estimte for the power-law index. For instance, in the case of woodland forest type of surface roughness, the suggested range of the roughness length in Ref. 32 is from 0.2 to 0.9 m (0.66 to 2.95 ft), i.e., a 450% change. The corresponding variation in the power-law index is from 0.25 to 0.33, i.e., a 32% difference. Similar changes in the power-law index are by and large obtained when the roughness-length ranges recommended in Ref. 6 are used. Such an approach cannot thus supply a reasonable estimate for the power-law index. In fact, one cannot isolate the effect of the surface roughness upon the power-law index from that of the wind conditions since the turbulence for a given surface roughness depends upon it. It is thus apparent that the effects of both the surface roughness and wind conditions upon determining the power-law index are to be concurrently considered.

4. POWER-LAW PARAMETERS

The lack of a consistent empirical method for the estimation of the two reference scales and the index of the power law is clearly indicated by the previous discussion of the main approaches currently used. Particularly noticeable is the inability of these methods to satisfactorily approximate the power-law index in terms of parameters characteristic of the surface roughness and the wind conditions. These methods are particularly lacking: (1) in advancing standard reference scales for a broad variety of surface roughnesses and a wide range of wind conditions; (2) in specifying the structure of any surface roughness in terms of a structure index; and (3) in describing the wind conditions by means of a single characteristic parameter. In fact, one cannot put forward a general empirical method for approximating the power-law index unless these three issues are first resolved.

4.1 Standard Reference Scales

In determining the reference height of the power law and its corresponding reference wind, it is necessary to consider the following criteria: (1) a height within which the production and most of the dissipation of turbulence occur; (2) a height which can be used for different types of surface roughness; (3) a height which can be readily measured and/or approximated; and (4) a height within which the wind shear undergoes its major variation. It is apparent that the height of the internal boundary layer, which is generated by the surface roughness, meets these basic conditions. Production of turbulence and the best part of its dissipation transpire in the internal boundary layer. Each particular surface roughness induces an internal boundary layer whose thickness can be roughly estimated. Most of the change in the wind shear with height is further confined within the internal boundary layer.

The thickness (or depth) of the internal boundary layer increases continuously with the streamwise distance from the front of the surface roughness until it reaches its full development. It grows similarly to the width of a two-dimensional wake that originates at the first upstanding row of roughness elements [10,12]. One then can approximate the streamwise growth of the thickness of the internal boundary layer δ_i as a function of the downstream distance x measured from the surface-roughness front by a power law of the form

$$\delta_i/h = C(x/h)^{\beta} , \qquad (4.1)$$

where h is the height of the surface roughness. Both the exponent β and the constant C in this power-law relationship depend, however, on the particular surface roughness being considered. This foregoing relationship approximates the growth of the internal boundary layer until its full development. The streamwise distance over which the internal boundary layer reaches its full development, denoted here by x_{fd}, is

usually determined based on the disappearance of the kink (viz., the change in the slope) in the mean wind variation with height. Essentially, one can view the fading of the kink in the mean wind variation as indicative of the adjustment of the turbulent shear stress induced by the surface roughness to that in the oncoming flow [12].

It is interesting to note that a power-law growth of the depth of the internal boundary layer formally similar to that advanced here was proposed in Ref. 9, assuming a logarithmic wind distribution throughout the internal boundary layer. The reference scale in this power law is the roughness length z_0 instead of the roughness height h used in Eq. (4.1). Moreover, the use of this power law is restricted starting from a downwind distance of at least 1000 roughness lengths from the surface roughness front. This downwind distance varies from 10 to 100 m for fine roughness where the roughness length z_0 is of the order of 0.01 to 0.1 m (see Fig. 3.2). In the case of high roughness, where typical values of the roughness length z_0 are larger than 1 m (see Fig. 3.2), this downwind distance can be as large as 1000 m or even larger.

The use of Eq. (4.1) in estimating the thickness of the internal boundary layer is contingent upon knowing the exponent β and the constant C for each type of surface roughness. At the present time, these two parameters are not known for each particular type of surface roughness because of the lack of sufficient and detailed data on the growth of the internal boundary layer. It is consequently suggested, at this stage, that only fine and high surface roughnesses be considered, since these two main categories provide a gross approximation for most types of surface roughness. In practice, one can distinguish between these two general classes according to the height of the roughness elements, which is commonly expressed in terms of the roughness length z_0, as indicated in Table 2 and in Fig. 3.2. Roughness elements of flat open country and moderately rough terrain are relatively short while those of woodland forest, urban area, rough terrain, and very rough terrain are higher. The corresponding values of the roughness length z_0 are either smaller or larger than 20 cm (0.656 ft), as illustrated in Fig. 3.2. In examining the type of roughness given in Table 2 for each class of surface roughness, it is further conceivable to consider roughness elements of a height smaller or greater than about 200 cm (6.56 ft) as being either short or high roughness elements. Accordingly, roughness elements shorter than 200 cm with a roughness length smaller than 20 cm are considered as fine surface roughness. Roughness elements higher than 200 cm with a roughness length larger than 20 cm are viewed as high surface roughness. This division into these two gross classes of surface roughness is indicated in Fig. 3.2. The same classification is applied to wind-tunnel type of surface roughness except when it represents a scaled-down model of either natural or man-made surface roughness. In the latter case, the height of the modeled roughness elements (viz., the height of the field roughness elements) and the corresponding scaled-up value of the roughness length z_0, according to the particular geometric scale, are used to classify the type of roughness. In addition, roughness elements of a height smaller than about 0.20 cm and of a roughness length smaller than 0.01 cm, say, such as in a rough pipe, are classified as very fine surface roughness. This third class of surface roughness is not shown in Fig. 3.2.

Characteristic values of the exponent β and the constant C in Eq. (4.1) for fine and high surface roughness can be deduced from field and/or wind-tunnel data. To this end, data on the growth of the internal boundary layer till its full development are needed. Such data are quite scarce in field situations. On the other hand, ample wind-tunnel data for these two general classes of surface roughness are available. Detailed wind-tunnel data on the growth of the internal boundary layer for flow over fine and high surface roughnesses are, for example, reported in Refs. 10 and 12, respectively. These wind-tunnel data can readily be employed to estimate characteristic values for the exponent β and the constant C. One then can use these estimates in Eq. (4.1) to obtain a first approximation of the fully developed thickness of the internal boundary layer whenever more reliable data are not available.

A growth of the internal boundary layer proportional to the streamwise distance to one-half power--i.e., $\delta_i \sim x$--was advanced in Ref. 10 for flow over fine surface roughness (rectangular slats of 0.3175 cm (1/8 in) square cross section and of 1.27 cm (1/2 in) pitch, i.e., "k-type" of roughness). This 1/2-power law was obtained by defining the outer edge of the internal boundary layer as the locus of the "knee" points (or kinks) in the mean velocity profiles. A value of 0.707 for the constant C was deduced from the data on the growth of the internal boundary layer reported in this reference (see Appendix III). Based on the fading of the knee point in the mean velocity profile with increasing streamwise distance, the internal boundary layer attained its full development in this flow at a downstream distance x_{fd} equal to about 80 to 100 roughness heights.

The values of the two parameters β and C in Eq. (4.1) for flow over high surface roughness were deduced from the wind-tunnel data reported in Ref. 12 (see Appendix III). Detailed results on the growth of the internal boundary layer in flow over a model forest canopy are presented in this reference. Relatively high plastic model trees (18 cm (7.1 in) in height) randomly and densely distributed (one roughness element per 46 cm^2 (7.13 in^2)) were used to model a forest canopy in this wind-tunnel study. The thickness of the internal boundary layer was determined based on the measured turbulent shear stress distribution with height. In fitting Eq. (4.1) to these data, values of 0.466 and 1.16 were obtained for the exponent β and the constant C,

respectively. Based on the turbulent shear stress variation [12] and on the evolution of the velocity along isoheights [45], the internal boundary layer reached its full development in this flow over a streamwise distance x_{fd} of about 30 to 40 roughness heights.

The foregoing values of the exponent β and the constant C are submitted as being representative for flow over fine and high surface roughness and are used as such hereinafter in estimating the fully-developed thickness of the internal boundary layer by means of Eq. (4.1). Their values along with the average streamwise distance (in terms of the roughness height h) within which the internal boundary layer fully develops--i.e., x_{fd}/h are summarized in Table 3 below:

TABLE 3. PARAMETERS OF EQ. (4.1)

Surface Roughness	β	C	x_{fd}/h
Fine	0.50	0.707	90
High	0.466	1.16	35

The additional parameter required in order to use Eq. (4.1) is the height of the surface roughness h. It can readily be measured when the roughness elements are of uniform height. In the case of roughness elements of nonuniform height, one can employ either an average or a median height. Consequently, Eq. (4.1) can be used to approximate the fully developed depth of the internal boundary layer for almost any type of surface roughness employing the values of β, C, and x_{fd}/h given in Table 3.

Selection of the thickness of the fully developed internal boundary layer as the reference height of the power law necessarily prescribes the corresponding reference wind U_1. The latter is the wind at the outer edge of the fully developed internal boundary layer. This reference wind accounts for the wind conditions within the internal boundary layer since it is determined by the wind-shear variation with height and the characteristics of the surface roughness. One can readily measure this reference wind since both the height δi and the streamwise distance x_{fd} where it transpires can be approximated by means of Eq. (4.1). The reference wind U_1 can even be measured at streamwise distances x greater than x_{fd} at the height δ_i prescribed by Eq. (4.1). This is consequent upon the relatively slow streamwise growth of the internal boundary layer after it reaches its full development [12]. In conclusion, it is proposed to use the height of the fully developed internal boundary layer δ_i and the wind there U_1 as the reference scales of the power law.

4.2 Surface-Roughness Structure Index

Specification of the structure of a surface roughness in terms of relevant length scales is of prime concern with regard to its overall effect upon the flow and, particularly, with respect to the total wall shear stress (i.e., the drag). Such a specification includes the shape of the roughness elements and their distribution. Roughness elements can be divided into two general classes according to their shape provided that their aeroelastic behavior is disregarded. Then the two categories of rigid roughness elements are: regular geometric shape and irregular shape. Examples of roughness elements of regular geometric shape are cubes, rectangular and/or square prisms, cylinders, spheres, spherical segments, truncated cones, and many other shapes. Such regular geometric shapes are generally used in modeling the real roughness elements encountered on earth's surface. Sand roughness, rocks, trees, bushes, shrubs, vegetative canopies and/or any other natural roughness, and man-made roughness (e.g., structures) are examples of irregular shapes that are usually found on earth's surface.

No general method for determining the characteristic dimensions of a three-dimensional roughness element of irregular shape has yet been introduced because of, in all likelihood, the extremely large variety in its form. It is, therefore, proposed that such roughness elements be modeled to a first approximation, by means of ideal square prisms of streamwise and transverse width s and uniform height h as portrayed in Fig. 4.1. The dimensions of such an ideal square prism can then be determined by imposing the conditions that its volume and height are equal to those of the irregular roughness element being modeled.

This proposed ideal square prism preserves the essential sharp corner separation characteristic of most three-dimensional natural and man-made roughness elements. Furthermore, this equivalent volumetric and height representation ensures the modeling of the global effect of the

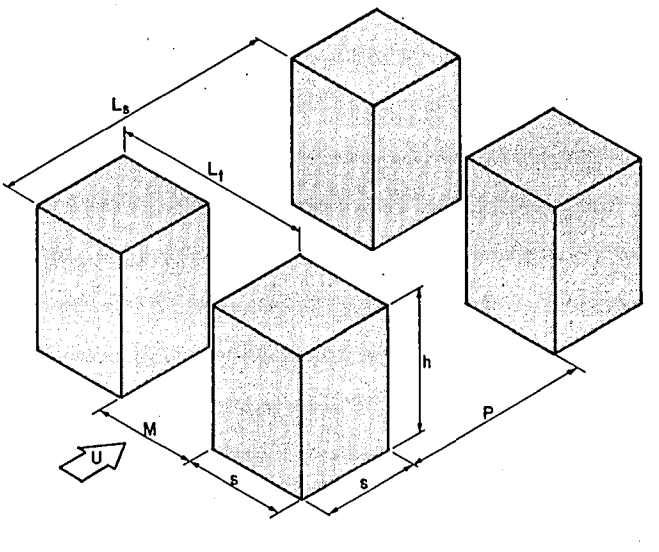

Figure 4.1.--Ideal surface roughness consisting of identical rigid square prisms of uniform height regularly distributed.

surface roughness on the flow. Any surface roughness is essentially an obstruction which forces the oncoming flow to split into two streams in order to adjust itself to the new surface conditions. Most of the flow is displaced upward above the new surface roughness to form an internal boundary layer. The rest of the flow is deflected inside the roughness where a variety of local flows develop depending upon the particular shape of the roughness elements. Both the upward displacement and the downward deflection of the flow are basically determined by the volume occupied by the surface roughness and by the height of the roughness elements. The height of the roughness elements plays an essential role in determining the depth of the internal boundary layer, as indicated by the distinction between fine and high surface roughness. Moreover, the wind shear and the turbulence within the internal boundary layer and the wall shear stress depend upon the roughness height. Higher roughness fosters a stronger wind shear, a higher level of turbulence, and a larger wall shear stress (or drag). Modeling of a tree (assuming that its stem is about 1/3 of its total height) and of a sand grain (or a rock) by ideal square prism of volume and height equal to those of the real elements is illustrated in Fig. 4.2.

Specification of the distribution of roughness elements over a given area--i.e., the number of elements per unit floor area--depends upon knowing the spacing between them in addition to their size. To this end, an ideal surface roughness consisting of an array of rigid similar square prisms of uniform height regularly spaced in both axial and transverse directions as depicted in Fig. 4.1 is considered. Whenever this

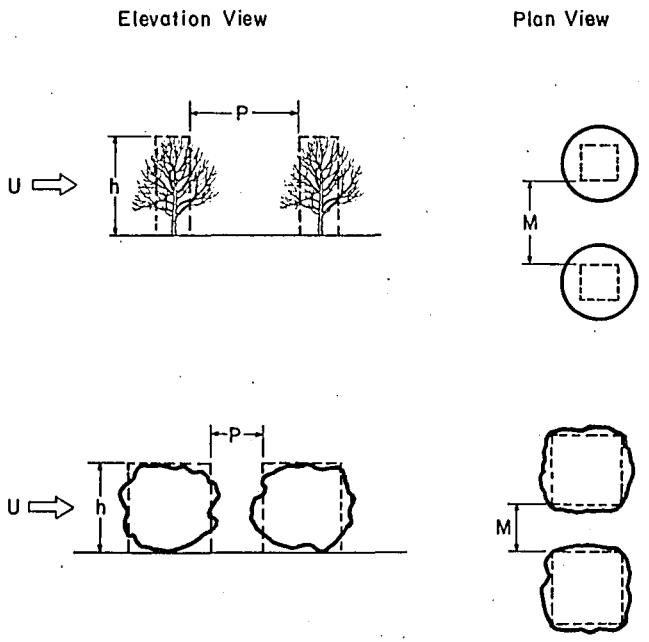

Figure 4.2.--Modeling of roughness elements of irregular shape by ideal prisms of volume and height equal to those of the real elements.

array represents a surface roughness consisting of roughness elements of different shape, the distribution of the ideal and the real roughness elements must be equal in order to preserve the characteristics of the flow. Array of staggered elements is not examined at this stage since it constitutes a more complex distribution. Then the significant spacings are the axial (or streamwise) and the transverse (or lateral) spacings denoted by pitch P and mesh M, respectively, which are shown in Fig. 4.1. One then can express the distribution of roughness elements in terms of their scales and of their pitch and/or mesh.

The pitch and the mesh play a prime role in determing the flow through the surface roughness and the wall shear stress (friction velocity or drag). Readjustment of the flow that separates from an upwind element to the presence of a downwind one transpires within the pitch. As a result, the wake of each element and the flow reattachment on the front face of a downstream element depend upon the pitch. A simplified qualitative description of the flow within the pitch region is portrayed in Fig. 4.3(a). The mesh determines the flow rate through the surface roughness and the development of the flow separation from the upwind corners of two adjacent elements. Interaction of the separation streamlines that spring from these corners and of the wakes of two adjacent elements along with the jet effect between them depend on the mesh. A gross illustration of these effects is given in Fig. 4.3(b).

The dimensions of the roughness elements and their pitch and mesh--i.e., the structure (or the architecture) of the surface roughness--determines the resistance to the flow and, hence, the total drag of the surface roughness. It is therefore important to specify each surface roughness by means of a structure index which accounts explicitly for those geometric scales that affect the flow the most. Apparently, the scales of prime interest are the height of the roughness elements and their pitch and mesh. At the present time, the volumetric density number [18], the

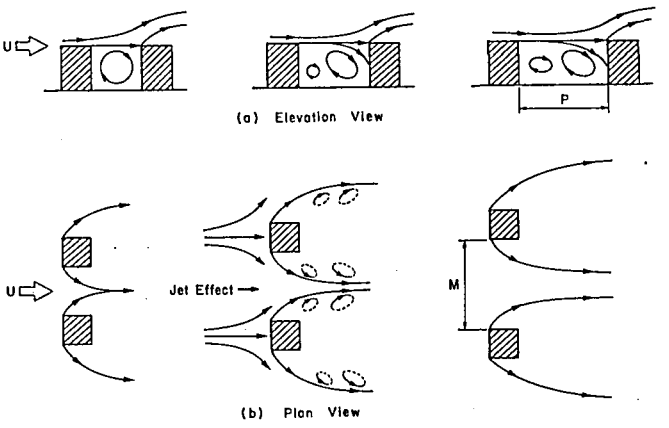

Figure 4.3.--Illustration of the flow pattern with varying (a) pitch and (b) mesh.

roughness density [46,47], and the roughness concentration [48,49] are used to describe the roughness structure. The volumetric density number, which is defined as the ratio of the net volume occupied by the roughness elements to the total volume of the surface roughness [18], represents a gross structure index. It indicates solely the overall effect of the surface roughness upon the flow rate. The architecture of the surface roughness is not explicitly accounted for by this index.

For two-dimensional roughness elements of uniform height and equally spaced, the roughness density is used as the roughness structure index. It is given by the ratio of the axial distance L_s between the leading edges of two successive elements (edge-to-edge streamwise distance) to the element's longitudinal width s (see Fig. 4.1), i.e., L_s/s [46,47]. The effect of the pitch P is included in this structure index since $L_s/s = 1 + P/s$. On the other hand, the height of the roughness element is not accounted for despite its importance with regard to the flow conditions above the roughness.

The structure index for three-dimensional roughness elements is expressed by the roughness concentration, which is defined as the ratio of the frontal area of each roughness element to its corresponding total floor area [48,49]. Thus, the roughness concentration is given by hs/L_sL_t, where L_s and L_t are the edge-to-edge streamwise and transverse distances between two successive and adjacent elements, as shown in Fig. 4.1. This surface-roughness structure index accounts for the element height. On the other hand, the pitch and the mesh are not appropriately considered despite their intrinsic significance. Changes in the streamwise and/or transverse width of the elements necessarily affect the pitch and/or the mesh while the two edge-to-edge distances (L_s and L_t) can remain unchanged. It is therefore suggested that the structure index be expressed in terms of the roughness elements height, pitch, and mesh by means of a geometric function of the form $\phi(h,P,M)$. At this stage, this geometric function can best be approximated by means of a simple dimensionless combination of these three scales given by

$$\lambda = \left(\frac{h}{P}\right)^{\eta} \left(\frac{h}{M}\right)^{\xi} \quad . \tag{4.2}$$

This structure index also applies to two-dimensional roughness elements, but then ξ must be zero since only the pitch is relevant in this case. The values of the two exponents η and ξ depend upon the architecture of the surface roughness being considered. No attempt to evaluate this dependence was undertaken in view of the large amount of detailed data required to accomplish this. In view of these circumstances, it is proposed that value of unity be assumed for these two exponents. Thus, the surface-roughness structure index is approximated herein by

$$\lambda = \frac{h}{P}\,\frac{h}{M} \quad , \tag{4.3}$$

for three-dimensional roughness elements. In the case of two-dimensonal roughness elements, the surface-roughness structure index reduces to

$$\lambda = h/P \quad , \tag{4.4}$$

where the pitch P is then the distance between two successive elements.

The foregoing surface-roughness structure index accounts at once for the scales and the distribution of the elements. The element scales are expressed by the height and by the prevailing pitch and mesh while the distribution is given by the latter two parameters. Changes in any of these three scales, which evidently affect the flow, are reflected in the value of this structure index. Higher elements for the same pitch and mesh produce, for instance, a larger available volume for the flow within the pitch and the mesh. Different pitch and/or mesh for the same element height can either increase or decrease the resistance of the surface roughness to the flow. One thus can view this structure index λ as an aspect ratio of the surface roughness. It is further important to notice that this structure index places emphasis on the roughness height h in view of its prominent role in determining the wind conditions within the internal boundary layer. This surface-roughness structure index was introduced based on physical premises and, therefore, further checking of its applicability for both field and wind-tunnel surface roughness is essential.

4.3 Wind Conditions

The wind shear and its strength--i.e., the wind conditions--within the internal boundary layer vary depending upon the particular surface roughness and the oncoming wind. Description of the wind conditions by means of a single characteristic parameter is consequently of prime interest. The natural choice for such a parameter is a Reynolds number defined in terms of a characteristic wind and a suitable length scale. It is evident that one can select the reference wind of the power law U_1 as the characteristic wind. This reference wind is the wind at the outer edge of the fully developed internal boundary layer and, hence, it is representative of the prevailing wind conditions in the internal boundary layer, as previously discussed in Sect. 4.1.

Either the thickness of the fully developed internal boundary layer given by Eq. (4.1) or a characteristic scale of the surface roughness can be employed as the length scale of a Reynolds number. The former is, as a matter of fact, indirectly accounted for by the reference wind and, therefore, its explicit use as a length scale is redundant. On the other hand, the use of a scale of the surface roughness as the length scale ensures that the influence of the surface roughness upon the wind conditions is indicated by the Reynolds number. The height of the surface roughness is employed to identify the general type of roughness and its effect upon the wind

conditions. Consequently, it is proposed that h be selected as the length scale. One then can characterize the wind conditions by a Reynolds number based on the reference wind U_1 of the power law and the height h of the surface roughness, i.e., by

$$Re = U_1 h/\nu \ , \qquad (4.5)$$

in which ν is the kinematic viscosity. One can furthermore view this reference-wind Reynolds number as indicative of the turbulence conditions and of the wall shear stress because of its characteristic wind and length scale.

4.4 Roughness-Wind Interaction Parameter

A structure index and a Reynolds number have thus far been advanced to separately describe the architecture of the surface roughness and the wind conditions. In order to simultaneously account for both of them, it is plausible to consider a combination of the foregoing two parameters. Such a compound parameter can be viewed as describing the interaction between the surface roughness and the wind. It is proposed, at this point, that such an interaction parameter be defined in terms of the product of the surface-roughness structure index and the reference-wind Reynolds number (see Eqs. (4.3) and (4.5)). Then the interaction parameter for three-dimensional surface roughness is approximated by

$$\lambda Re = \frac{h}{P}\,\frac{h}{M}\,\frac{U_1 h}{\nu} \ . \qquad (4.6)$$

In the case of two-dimensional roughness elements, the interaction parameter reduces to

$$\lambda Re = \frac{h}{P}\,\frac{U_1 h}{\nu} \ , \qquad (4.7)$$

since then the structure index λ is given by h/P (see Eq. (4.4)). It is important to point out that the interaction parameter stresses the role of the height of the surface roughness since it is proportional to h^3 and to h^2 for three- and two-dimensional surface roughness, respectively. This dependence on the roughness height underscores, in fact, the effect of very fine, fine, and/or high roughness upon the wind variation and turbulence. Generally, a larger interaction parameter indicates both higher roughness elements and stronger wind.

Insofar as the power law is concerned, higher surface roughness and/or stronger reference wind lead generally to a larger power-law index. To date, these two effects were considered separately, as outlined in Sect. 3. It is therefore desirable to explore whether one can relate the power-law index to the roughness-wind interaction parameter. Such a relationship would simultaneously account for both the surface roughness structure and the wind conditions.

5. POWER-LAW INDEX ESTIMATION

5.1 Power-Law Index Range

Basically, the power-law index can take on any value between zero and unity depending on the structure of the surface roughness and the wind conditions, as previously mentioned. The two extremes values of zero and unity correspond to uniform wind and linear wind shear, respectively, as is observed by simple inspection of Eq. (3.1). These two extreme values are, in fact, never assumed by the power-law index.

A range for the power-law index can readily be determined by considering the momentum thickness [14]

$$\theta = \int_0^\infty \frac{U}{U_1}\left(1 - \frac{U}{U_1}\right)dz \ , \qquad (5.1)$$

which expresses the loss of momentum within the boundary layer as compared with potential flow. In the foregoing equation z is the height, while the local wind and the reference wind are denoted by U and U_1, respectively. Substitution of the power law for U/U_1 given by Eq. (3.1) into Eq. (5.1) and subsequent integration up to the outer edge of the internal boundary layer δ_i lead to the following result [50]

$$\theta/\delta_i = \frac{\alpha}{(\alpha + 1)(2\alpha + 1)} \ . \qquad (5.2)$$

Variation of the dimensionless momentum thickness θ/δ_i (i.e., the momentum thickness for any given internal boundary layer thickness δ_i) with increasing power-law index according to Eq. (5.2) is displayed in Fig. 5.1. One can clearly observe that the dimensionless momentum thickness reaches a maximum for a power-law index of 0.707. The latter represents, as a matter of fact, the largest value that the power-law index can take on.

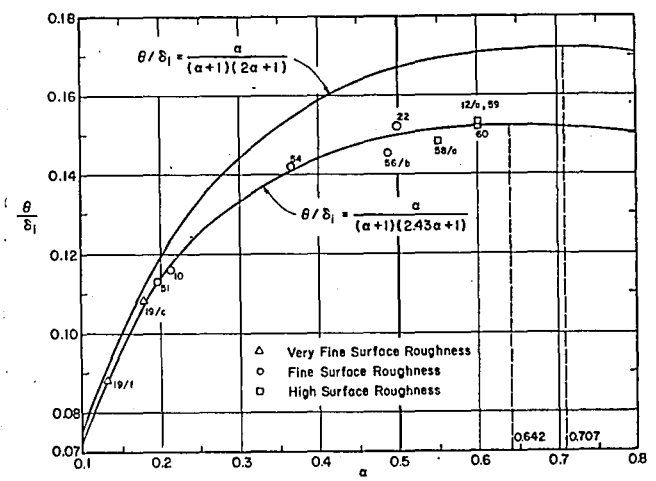

Figure 5.1.--Variation of the dimensionless momentum thickness with increasing power-law index.

To date, the available approximations for the power-law index indicate that its largest value is smaller than that suggested by the maximum momentum thickness. This is manifested by the empirical correlations relating the power-law index either to the 10 m height reference wind or to the roughness length shown in Figs. 3.1 and 3.2. Examination of these two correlations reveals that the power-law index varies from 0.19 to 0.31 with increasing 10 m height reference wind (see Fig. 3.1) and from about 0.1 to 0.4 with higher roughness length (see Fig. 3.2). No upper limit for the power-law index is advanced in either one of these two empirical correlations. The decrease in the power-law index with increasing 10 m height reference wind advocated by Eq. (3.3) is discarded since this trend is in conflict with all known results except for those reported by its proponents in Ref. 42.

5.2 Method for Power-Law Index Estimation

In a turbulent boundary layer at zero pressure gradient, such as an internal boundary layer, the momentum thickness at any given streamwise station is proportional to the local wall shear stress (or friction velocity) [14]. The latter depends on the architecture of the surface roughness and the wind conditions. A single roughness-wind interaction parameter given by Eq. (4.6) was introduced in order to concurrently account for these two factors. A higher surface roughness and/or a stronger wind produce more turbulence and, hence, a larger local wall shear stress. In turn, the latter induces a greater momentum thickness which promotes a higher power-law index according to Eq. (5.2) and as shown in Fig. 5.1. A theoretical description of this complex process is not yet feasible in view of the inherent limitations associated, for that matter, with modeling of a turbulent boundary layer over a rough surface. It is apparent, on the other hand, that the dependence of the power-law index upon the roughness-wind interaction parameter can be expressed by means of a suitable empirical correlation. Within the context of such a correlation, the power-law index is necessarily bounded by its maximum value of 0.707 prescribed by the momentum thickness variation according to Eq. (5.2) (see Fig. 5.1). The roughness-wind interaction parameter can, on the other hand, take on any value since it is not limited by an upper bound. As a result, one can expect that the power-law index would asymptotically approach its maximum value with increasing interaction parameter.

In order to advance a correlation between the power-law index and the interaction parameter, it is necessary to include data encompassing a wide range of the latter in view of the finite range of the former. Since the interaction parameter is given in terms of the surface-roughness structure index λ and the reference-wind Reynolds number Re (see Eqs. (4.6) and (4.7)), it is essential to use values of these two factors varying within several orders of magnitude. The structure index is defined in terms of the height, pitch, and mesh of the roughness elements (see Eqs. (4.3) and (4.4)) while the Reynolds number is based on the reference wind and the height of the roughness elements (see Eq. (4.5)). Values of the structure index and Reynolds number varying over a large range can be obtained by considering very fine, fine, and high roughness elements of a variety of geometric shapes (i.e., regular and irregular shapes) and distributions, and a wide range of the reference wind. This can be accomplished by examining data collected in wind-tunnel and field investigations over a great range of surface roughnesses and wind conditions.

Based on an extensive, albeit not exhaustive, survey of reported data, a rough pipe flow [19], eight wind-tunnel [10,12,51,52,53,54,57,58] and five field [22,55,56,59,60] investigations were selected. Data for different roughness heights and/or wind conditions were reported in several studies [12,19,53,56,57,58]. Insofar as the classification of the surface roughness as very fine ($h < 0.2$ cm and $z_0 < 0.01$ cm), fine ($h \cong 0.2$ - 200 cm and $z_0 < 20$ cm), and high ($h > 200$ cm and $z_0 > 20$ cm) is concerned (see Sect. 4.1), the selected data include six cases for very fine surface roughness [19/a through 19/f], ten cases for fine surface roughness [10,22,51,52,53/a,53/b,54,55,56/a,56/b], and eight cases for high surface roughness [12/a, 12/b,57/a,57/b,58/a,58/b,59,60]. Thus, data for twenty-four different cases were compiled. The six very fine surface roughness cases [19/a through 19/f] are for flow over three different roughness heights when data for two different velocities for each roughness height were chosen. In the wind-tunnel investigation of flow over fine surface roughness reported in Ref. 53, roughness elements of the same regular geometric shape but of different heights were used. Data only for the flow over the shortest [53/a] and the highest [53/b] roughness elements were used herein. The data reported in Ref. 56 were collected in two different field studies of flow over fine surface roughness. In each of the three wind-tunnel investigations of flow over high surface roughness [12,57,58], data for two different cases were compiled. These six cases differ in the distribution and/or shape of roughness elements, and in the wind conditions. All the twenty-four cases are listed according to their class--i.e., very fine, fine, and high surface roughness--and with increasing height of the roughness elements within each class in Table 4 below. The kind, type (i.e., two-dimensional (2D) or three-dimensional (3D)), and height h of the roughness elements, the corresponding roughness length z_0, and the experimental environment (i.e., pipe flow, wind tunnel or field) are also given in Table 4. All the details concerning the characteristics of each surface roughness and the estimation of the roughness length are outlined in Appendix IV.

The six wind-tunnel cases included in the high surface roughness class are simulation studies of flow above models of a forest canopy [12/a,12/b], an ideal forest canopy [57/a,57/b],

TABLE 4. SURFACE ROUGHNESS DATA

Surface Roughness Class	Source	Ref. No.	Roughness Elements: Kind	Type	Height (cm)	z_0 (cm)	Experimental Environment
Very fine	Nikuradse	19/f	Sand grains	3D	0.0098	0.0005	Pipe flow
		19/e				0.0006	
		19/d			0.02	0.0002	
		19/c				0.0005	
		19/b			0.08	0.003	
		19/a				0.004	
Fine	Furuya et al.	51	Wires	2D	0.2	0.010	Wind tunnel
	Antonia & Luxton	10	Square bars	2D	0.3175	0.045	Wind tunnel
	Moore	53/a	Square bars	2D	0.3276	0.125	Wind tunnel
	Yeh & Nickerson	52	Gravel	3D	0.635	0.078	Wind tunnel
	Mulhearn	54	Gravel	3D	1.45	0.038	Wind tunnel
	Moore	53/b	Square bars	2D	3.89	0.60	Wind tunnel
	Pasquill	22	Grass	3D	7.5	0.66	Field
	Blackadar et al.	55	Hay	3D	20	3.50	Field
	Carl et al.	56/a	Sagebrush	3D	100	16.50	Field
		56/b	Low vegetation		150	17.50	
High	Ito	58/a	Pegs	3D	508	35	Wind tunnel
	Kawatani & Meroney	57/a	Pegs	3D	900	29	Wind tunnel
		57/b	Pegs		900	76	
	Ito	58/b	Plastic strips	3D	1016	43	Wind tunnel
	Kawatani & Sadeh	12/a	Plastic trees	3D	1800	84	Wind tunnel
		12/b			1800	175	
	Jungle Canopy	59	Jungle canopy	3D	3000	125	Field
	Shinn	60	Gum-maple forest	3D	3100	23	Field

and tall vegetation [58/a,58/b]. These wind-tunnel investigations represent, in practice, modeling of flow above field roughness elements of a height ranging from 508 to 1800 cm based on a geometric scale of about 1:100, which is commonly used in scaling down natural high roughness [18]. The height of the field roughness elements and the scaled-up values of their roughness lengths (1:100) are listed in Table 4 above in order to point out their high roughness nature.

5.3 Wind-Shear Data Examination

A detailed examination of the wind-shear data reported in the 24 cases listed in Table 4 was conducted for the purpose of exploring the feasibility of correlating the power-law index with the roughness-wind interaction parameter. The procedure in carrying out the computation of the various parameters needed for obtaining the desired correlation consists of the following five steps:

(1) Determination of the standard reference scales of the power law, i.e., reference height and wind, z_1 and U_1.

(2) Approximation of the surface-roughness structure index λ.

(3) Computation of the reference-wind Reynolds number Re.

(4) Computation of the roughness-wind interaction parameter λRe.

(5) Estimation of the power-law index α.

A brief review of how these parameters were estimated and/or computed is given herein in order to point out the various approximations used. All the details on the data employed in each case for determining the standard reference scales and for estimating the structure index are given in Appendix IV, which also gives the wind-shear data reported in each case.

The standard reference height of the power law, which is the height (or thickness) of the fully developed internal boundary layer δ_i as outlined in Sect. 4.1, is denoted here by z_1 for consistency with the accepted notation. In flow above fine and high surface roughness, the reference height was estimated by means of Eq. (4.1), using the corresponding values of its parameters (viz., β, C, and x_{fd}/h) advanced in Table 3 (see Sect. 4.1). Then the reference height z_1 is given by 6.707h and 6.081h for fine and high surface roughness, respectively (h is the height of the roughness elements). The standard reference wind U_1, which is the wind at the reference height z_1, was estimated in each case from the reported wind data within the fully developed internal boundary layer. It was deduced from wind-shear data at streamwise

distances roughly equal to [12/a,12/b,51,52, 53/a,53/b,54,55,57/a,57/b,58/a,58/b] or greater [10,22,56/a,56/b,59,60] than x_{fd}/h depending upon the available data. The streamwise distance over which the internal boundary layer attains its full development x_{fd}/h varies from about 80 to 100 and from 30 to 40 for flow over fine and high surface roughness, respectively, as previously indicated in Sect. 4.1. In addition, the reference wind was estimated by vertical extrapolation of the given wind shear in two field cases [59,60] because of lack of data at the required reference height.

All the six cases of flow above very fine surface roughness are based on data reported in a comprehensive investigation of fully developed water flow through a rough pipe [19a through 19f]. The characteristic length for this flow situation is the thickness of the fully developed turbulent boundary layer, which is equal to the pipe radius (measured from the wall) and not the thickness of the internal boundary layer. Consequently, the thickness of the fully developed boundary layer and the velocity along the pipe axis (i.e., the maximum velocity) are the standard reference height z_1 and velocity U_1, respectively, for this flow.

The surface-roughness structure index λ introduced in Sect. 4.2 is a parameter that specifies the architecture of the surface roughness, i.e., the height and distribution of the roughness elements. It is expressed in terms of the height h, pitch P, and mesh M for three-dimensional roughness elements and in terms of solely the height h and pitch P for two-dimensional roughness elements. The height of the roughness elements was reported in all the studies except one single case [56/a]. In this latter case, the height of the roughness elements was assumed based on inspection of similar roughness cover. On the other hand, the pitch and mesh, which are the streamwise and transverse spacings between two roughness elements (see Figs. 4.1 and 4.2), were approximated in each case based on whatever information concerning the shape and distribution of the roughness elements was supplied.

In the cases where the surface roughness consisted of two- or three-dimensional roughness elements of regular geometric shape uniformly distributed [10,51,53/a,53/b,57/a,57/b,58/a,58/b], the pitch and mesh were determined based on the given center-to-center (or edge-to-edge) spacing between two roughness elements and the dimensions of the element. Note that for two-dimensional roughness elements [10,51,53/a,53/b] the pitch is the sole relevant spacing. For three-dimensional roughness elements of equal sides, the pitch and mesh are equal because of their uniform distribution [57/a,57/b,58/a]. In a single case [58/b], the pitch and mesh are different since the sides of the roughness elements (rectangular strip) were unequal. Roughness elements of irregular shape with sharp corners randomly distributed [12/a,12/b,52,54] were modeled by ideal square prisms uniformly distributed as proposed in Sect. 4.2 (see Figs. 4.1 and 4.2). The sides and height of the equivalent ideal square prism were computed based on the conditions that its volume and height are equal to those of the real roughness elements. Next, the center-to-center spacing among the uniformly distributed square prisms was approximated under the condition that their distribution (viz., number of elements per unit area) is equal to that of the real roughness elements (which was given). The pitch (and equal mesh) was then estimated in the same manner as for the roughness elements of regular geometric shape.

For the tree elements reported in Refs. 59 and 60, the pitch (and mesh) was taken equal to the given mean spacing between two trees because of lack of information concerning the various dimensions of the trees. In using this approximation it was, in fact, implied that this mean spacing is representative of the uniformly distributed equivalent square prisms. In four field cases [22,55,56/a,56/b], the pitch (and mesh) was simply assumed based on the sketchy description given of the surface roughness and on inspection of similar roughness covers with the assumption of roughness elements uniformly distributed. These estimates were used despite their conjectural nature because of the lack of better information.

Finally, the sand grains used in the rough pipe flow experiment were modeled by identical spheres of diameter equal to their average height and uniformly distributed as recommended in Ref. 19. Their pitch (and equal mesh) was consequently approximated in the same way as for the roughness elements of regular geometric shape. With the completion of the approximations of the pitch (and mesh), the surface-roughness structure index λ was computed in each case by means of Eq. (4.3) or (4.4) for three- or two-dimensional roughness elements, respectively.

The reference-wind Reynolds number was advanced in order to describe the wind conditions within the internal boundary layer by means of a single characteristic parameter (see Sect. 4.3). This characteristic Reynolds number, which is based on the reference wind U_1 and the height h of the roughness elements, was computed for each case according to Eq. (4.5). In computing the reference-wind Reynolds number, kinematic viscosities ν of 10^{-6} and 1.5×10^{-5} m^2/s (at 20°C and standard pressure) were adopted for water [19/a through 19/f] and air (all the other cases), respectively, for standardization's sake. The order of magnitude of the Reynolds number is, in all likelihood, not affected by using these standard values for the kinematic viscosity.

In order to characterize the interaction between the surface roughness and the wind, the roughness-wind interaction parameter was put forward (see Sect. 4.4). This interaction parameter, which is given by the product of the surface-roughness structure index λ and the reference wind Reynolds number Re, was computed by means of Eqs. (4.6) and (4.7) for three- and two-dimensional roughness elements, respectively.

The last step consists of estimating the power-law index α. To this end, a power-law variation according to Eq. (3.1) was fitted in each case to the given wind-shear data using the corresponding standard reference height z_1 and wind U_1. This curve fitting was carried out graphically by plotting the change in the dimensionless wind shear U/U_1 with increasing dimensionless height z/z_1 on logarithmic paper, in view of its expediency and acceptable accuracy. The variations of the wind shear with height for flow above very fine, fine, and high surface roughness are displayed in Figs. 5.2, 5.3, and 5.4, respectively. Inspection of these best faired curves indicates that the wind shear is satisfactorily described in each case by a power law. Then the power-law index α, which is given by the slope of each curve, was deduced in each case from these best fitted curves.

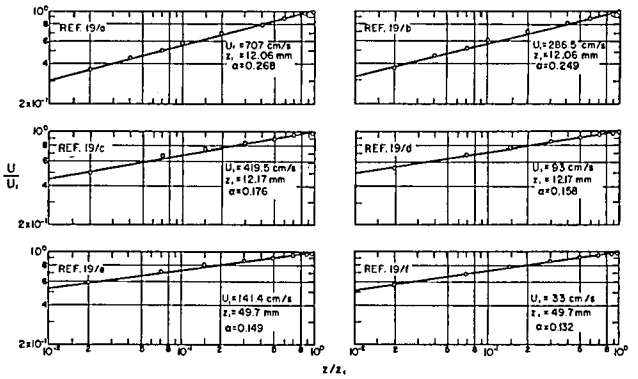

Figure 5.2.--Wind-shear variation over very fine surface roughness.

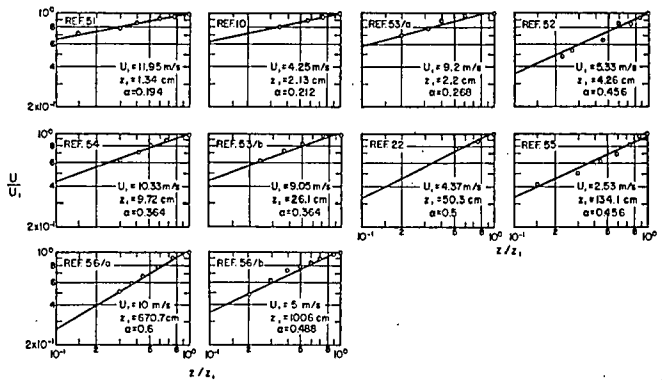

Figure 5.3.--Wind-shear variation over fine surface roughness.

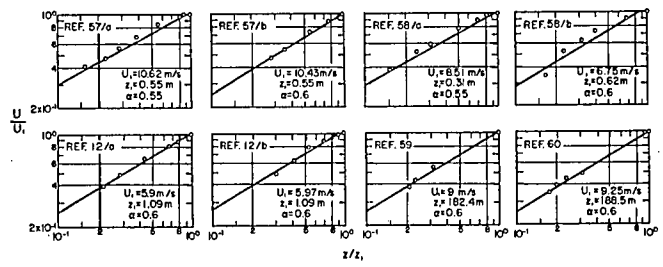

Figure 5.4.--Wind-shear variation over high surface roughness.

The results obtained by applying the method outlined above to the data selected (see Table 4) are summarized in Tables 5, 6, and 7 below for flow above very fine, fine, and high surface roughness, respectively. In these three tables the various parameters are tabulated with increasing reference height z_1. The values of the parameters given for the six wind-tunnel cases of flow above high surface roughness [12/a, 12/b,57/a,57/b,58/a,58/b] are for the wind-tunnel simulated flow and the corresponding model surface roughness. Since these wind-tunnel flows apparently met the condition of geometric and kinematic similarity, the value of the power-law index is the same for both the wind-tunnel simulated flow and the corresponding field flow. Recall that in wind-tunnel modeling of flow over high surface roughness, the condition of equal Reynolds number is relaxed [2].

Inspection of the results given in the three tables below reveals that the data encompass, as expected, wide ranges of surface roughnesses and wind conditions. These wide ranges are indicated by the variations of the surface-roughness structure index λ, the reference-wind Reynolds number Re, and the roughness-wind interaction parameter λRe for each class of surface roughness. For the six very fine surface roughness cases (Table 5), the structure index is the same (0.44) because of the particular changes in the height, pitch, and mesh of the roughness elements, i.e., the surface-roughness architecture. On the other hand, the Reynolds number varies from 32 to 5660 and the interaction parameter ranges from 14 to 2490. In the ten fine surface roughness cases (Table 6), the structure index ranges from 0.14 to 13.09, the Reynolds number changes from 900 to 6.7×10^5, and the interaction parameter varies from 224 to 1.2×10^6. Finally, for the eight high surface roughness cases (Table 7), the structure index changes from 3.83 to 64, the Reynolds number from 2.9×10^4 to 1.9×10^7, and the interaction parameter ranges from 1.8×10^5 to 1.2×10^9.

Classification of surface roughness as very fine, fine, or high was determined here based primarily on the height of the roughness elements. The height range for each class was further advanced based on the type of surface roughness and corresponding roughness length (see Sect. 4.1). It is, therefore, interesting to examine the variations of the structure index, Reynolds number, and interaction parameter with increasing height of the roughness elements.

A clearly discernible increase in the structure index with increasing height of the roughness elements cannot generally be expected in view of its intrinsic definition. The structure index is a dimensionless parameter which describes the architecture of each particular surface roughness in terms of its geometric characteristics, viz., in terms of the ratio of the height to pitch and mesh or the ratio of the height to the pitch for three- or two-dimensional roughness elements (see Eqs. (4.3) and (4.4)). Recall that the pitch and mesh account for the distribution of the roughness elements. To start

TABLE 5. PARAMETERS FOR FLOW OVER VERY FINE SURFACE ROUGHNESS

Source	Ref. No.	z_1 (mm)	U_1 (cm/s)	h (mm)	P (mm)	M (mm)	λ	Re	λRe	α
Nikuradse	19/a	12.06	707.0	0.8	1.2	1.2	0.44	5660	2490	0.268
	19/b		286.5					2290	1008	0.249
	19/c	12.17	419.5	0.2	0.3	0.3	0.44	839	369	0.176
	19/d		93.0					186	82	0.158
	19/e	49.7	141.4	0.098	0.147	0.147	0.44	139	61	0.149
	19/f		33.0					32	14	0.132

TABLE 6. PARAMETERS FOR FLOW ABOVE FINE SURFACE ROUGHNESS

Source	Ref. No.	z_1 (cm)	U_1 (m/s)	h (cm)	P (cm)	M (cm)	λ	Re	λRe	α
Furuya et al.*	51	1.34	11.95	0.2	1.4	*	0.14	1.6×10^3	224	0.194
Antonia & Luxton*	10	2.13	4.25	0.3175	0.9525	*	0.33	900	297	0.212
Moore*	53/a	2.20	9.20	0.3276	0.95	*	0.34	2×10^3	680	0.268
Yeh & Nickerson	52	4.26	5.33	0.635	0.1755	0.1755	13.09	2.3×10^3	3×10^4	0.456
Mulhearn	54	9.72	10.33	1.45	2.09	2.09	0.48	10^4	4.8×10^3	0.364
Moore*	53/b	26.10	9.05	3.89	11.3	*	0.34	2.3×10^4	7.8×10^3	0.364
Pasquill	22	50.30	4.37	7.5	3.5	3.5	4.59	2.2×10^4	10^5	0.50
Blackadar et al.	55	134.10	2.53	20.0	20.0	20.0	1.0	3.4×10^4	3.4×10^4	0.456
Carl et al.	56/a	670.70	10.00	100.0	75.0	75.0	1.78	6.7×10^5	1.2×10^6	0.60
	56/b	1006.00	5.00	150.0	375.0	375.0	0.16	5×10^5	8×10^4	0.488

*Two-dimensional roughness elements

TABLE 7. PARAMETERS FOR FLOW ABOVE HIGH SURFACE ROUGHNESS

Source	Ref. No.	z_1 (m)	U_1 (m/s)	h (cm)	P (cm)	M (cm)	λ	Re	λRe	α
Ito	58/a	0.31	8.51	5.08	2.06	2.06	6.08	2.9×10^4	1.8×10^5	0.55
Kawtani & Meroney	57/a	0.55	10.62	9.0	4.6	4.6	3.83	6.4×10^4	2.4×10^5	0.55
	57/b	0.55	10.43	9.0	2.06	2.06	19.09	6.3×10^4	1.2×10^6	0.60
Ito	58/b	0.62	6.75	10.16	5.08	1.9	10.69	4.6×10^4	4.9×10^5	0.60
Kawatani & Sadeh	12/a	1.09	5.90	18	6.1	6.1	8.71	7.1×10^4	6.2×10^5	0.60
	12/b	1.09	5.97	18	3.3	3.3	29.75	7.2×10^4	2.1×10^6	0.60
Jungle Canopy	59	182.4	9.00	3000	375	375	64.00	1.8×10^7	1.1×10^9	0.60
Shinn	60	188.5	9.25	3100	390	390	63.18	1.9×10^7	1.2×10^9	0.60

with, one can expect increasing values of the structure index with higher roughness elements since it is proportional to h^2 and h for three- and two-dimensional roughness elements, respectively. Changes in the pitch and mesh of roughness elements of a given height can, at the same time, drastically lessen or heighten the structure index. As a result, the structure index can take on almost any value, including equal values, for roughness elements of different heights, subject concurrently to an irregular increase in its value with higher roughness elements. Such a behavior of the structure index is manifested by the results presented in Tables 5, 6, and 7. For instance, the structure index for all very fine surface roughness cases is the same since the decrease in the height of the roughness elements is accompanied by a reduction in their pitch and mesh. This indicates that the architecture of these six surface roughnesses is the same despite changes in their height and distribution. Structure indexes for four fine surface roughness cases [10,51,53/a, 53/b] smaller than those for very fine surface roughness were obtained. Similarly, in four high surface roughness cases [12/a,57/a,58/a,58/b], lower structure indexes than that for a fine surface roughness case [52] were found. Such smaller structure indexes for higher roughness elements are consequent upon their distribution (i.e., pitch and mesh) in each particular case.

The Reynolds number is directly proportional to both the height of the roughness elements and

the reference wind (see Eq. (4.5)). One thus can expect a greater Reynolds number as the roughness elements are higher, provided that the reference wind is roughly of constant strength. On the other hand, the Reynolds number for flow above roughness elements of a given height can take on a variety of values depending upon the prevailing reference wind. Such variations in the Reynolds number are revealed by the results given in Tables 5, 6, and 7. The Reynolds numbers for the six very fine surface roughness cases exhibit an increase by two orders of magnitude as both the height of the roughness elements and the reference velocity become larger. For the fine and high surface roughness cases, the Reynolds number increases randomly with higher roughness elements. The lack of smooth increase in the Reynolds number results from the variations in the prevailing reference wind in each case. For four fine surface roughness cases [10,51,52, 53/a], the Reynolds numbers are smaller than or equal to their counterparts for two very fine surface roughness cases [19/a,19/b] despite the reference wind-height product being larger in the former four cases. This is because of the difference in the kinematic viscosities of the fluids, viz., air in the former four cases and water in the latter two cases. The Reynolds numbers for the six wind-tunnel cases included in the high surface roughness class [12/a, 12/b,57/a,57/b,58/a,58/b] are smaller than some of their counterparts for fine surface roughness [56/a,56/b] since they were based on the wind-tunnel data as previously mentioned.

The interaction parameter is given by the product of the structure index and the Reynolds number (see Eqs. (4.6) and (4.7)) and, therefore, its variation with increasing height of the roughness elements is essentially similar to that of its two factors. Examination of the results presented in Tables 5, 6, and 7 indicates such a variation. As the roughness elements are higher the interaction parameter increases subject, as expected, to the same scattering found for the structure index and the Reynolds number.

The important aspect of the changes in the structure index, the Reynolds number, and the interaction parameter is their increasing values with higher roughness elements notwithstanding the lack of a smooth pattern. One cannot expect, as a matter of fact, a continuous increase in the values of these three parameters with the height of the roughness elements because of the random changes in the factors used in computing them. In conclusion, it is apparent that these three parameters can be used to characterize the surface roughness and wind condition within each surface roughness class despite the associated intrinsic limitations.

5.4 Power-Law Index Variation

Generally, an increase in the power-law index with increasing height of roughness elements is expected. Such a behavior is based on the known increase in the power-law index with larger roughness length (see Fig. 3.2). Recall that the roughness length is indicative of the height of the surface roughness. A smooth increase in the power-law index with higher roughness elements cannot be anticipated since its value in each case also depends upon the particular surface roughness architecture (viz., the structure index) and the prevailing wind conditions (viz., the Reynolds number). As a result, the power-law index can take on identical values for roughness elements of different heights or can assume different values for roughness elements of the same height notwithstanding its basic trend of becoming larger with higher roughness elements.

Examination of the values for the power-law index given in Tables 5, 6, and 7 reveals that they range between 0.132 and 0.268 for very fine surface roughness, between 0.194 and 0.60 for fine surface roughness, and between 0.55 and 0.60 for high surface roughness. This variation of the power-law index α with increasing height h of roughness elements is portrayed in Fig. 5.5. Each case is designated in this figure by its reference number. The height ranges for the three classes of surface roughness are also delineated in this figure. Note that for the six wind-tunnel cases of flow above high surface roughness [12/a,12/b,57/a,57/b,58/a,58/b], the height of the corresponding field roughness elements given in Table 4 was used. A consistent increasing pattern in the power-law index with higher roughness elements is discerned despite the associated relatively large scattering. This scattering results from obtaining: (1) a same power-law index for roughness elements of different heights, (see cases 19/a and 53/a; 52 and 55; 53/b and 54; 12/a, 12/b, 56/a, 57/b, 58/b, 59, and 60; 57/a and 58/a); (2) different power-law indexes for roughness elements of same height, (see cases 19/a and 19/b; 19/c and 19/d; 19/e and 19/f); and (3) a smaller power-law index with increasing height, (see cases 10, 51 vs. 19/a, 19/b; 53/b, 54 vs. 52; 55 vs. 22; 56/b vs. 56/a). These variations in the power-law index are caused by changes in the structure index and/or the Reynolds number which are reviewed later. Further examination of the variation of the power-law index reveals that it reaches asymptotically a maximum value of about 0.60 with increasing height of the roughness elements.

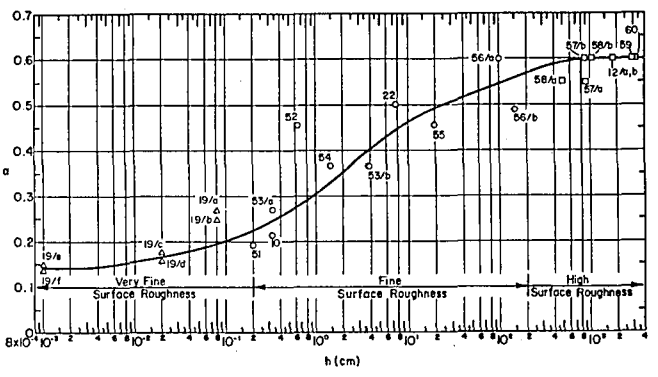

Figure 5.5.--Variation of the power-law index with increasing height of roughness elements.

In view of the commonly accepted method of representing the dependence of the power-law index upon the surface roughness in terms of the roughness length, as outlined in Sect. 3.2 and shown in Fig. 3.2 [6,32], the variation of the power-law indexes obtained here (Tables 5, 6, and 7) with their corresponding roughness lengths (Table 4) is displayed in Fig. 5.6. Note that the roughness length ranges for the three classes of surface roughness are marked off in this figure for convenience and that each case is denoted by its reference number. One can readily observe that the variation of the power-law index α with increasing roughness length z_0 is basically identical to that with increasing height of roughness elements displayed in Fig. 5.5. The power-law index exhibits with larger roughness length an increasing pattern in its value up to a maximum of 0.6, similar to its increase with increasing height of the roughness elements. A similar increasing pattern is also indicated by the variations of the power-law index with increasing roughness length according to the empirical equations (3.4) and (3.5) which are portrayed in Fig. 3.2. Despite this general similarity, these two relationships fail to suggest a maximum value for the power-law index, as observed in Fig. 5.6. It is further interesting to note that if the power-law index is approximated by the curve shown in Fig. 5.6, its value at any roughness length would be greater than that of its counterparts given in Fig. 3.2. This behavior can, in all likelihood, be attributed to the different reference scales of the power law employed in these two cases. The power-law index shown in Fig. 3.2 applies when the geostrophic height and wind are the reference scales of the power law. On the other hand, the reference scales employed for the power-law index portrayed in Fig. 5.6 are the height of the fully developed internal boundary layer and the wind there.

Inspection of the change in the power-law index with both increasing height of the roughness elements and higher roughness length displayed in Figs. 5.5 and 5.6 reveals, as mentioned above, that it attains asymptotically a maximum value of about 0.60. A similar increase in the power-law index up to a maximum of 0.707 was found based on the change in the momentum thickness within the internal boundary layer shown in

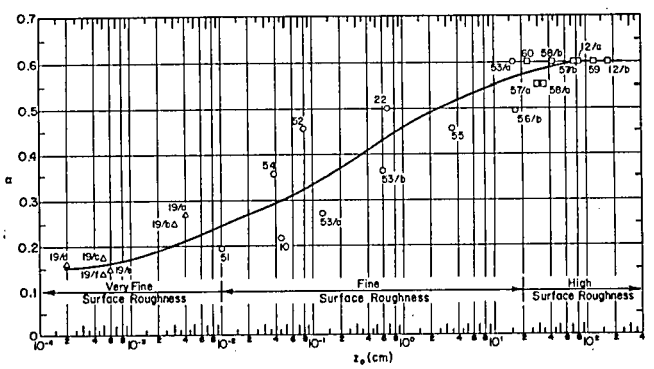

Figure 5.6.--Variation of the power-law index with increasing roughness length.

Fig. 5.1 (see Eq. (5.2) in Sect. 5.1). In view of this similar behavior, an examination of how the power-law indexes obtained here (see Tables 5, 6, and 7) vary with the momentum thickness of the corresponding internal boundary layers was undertaken. This examination was conducted for eleven representative cases which consisted of two very fine surface roughness [19/c,19/f], five fine surface roughness [10,22,51,54,56/b], and four high surface roughness [12/a,58/a,59,60] cases. In selecting these eleven cases attention was paid: (1) to encompass the entire power-law index range from 0.132 [19/f] to 0.60 [12/a,59, 60]; (2) to include cases for each particular experimental environment, e.g., two rough pipe flows [19/c,19f], five wind-tunnel flows [10, 12/a,51,54,58/a] and four field flows [22,56/b, 59,60]; and, (3) to include two-dimensional surface roughness cases [10,51].

The momentum thickness θ was estimated in each case by means of Eq. (5.1) which used the reported wind shear data for integration over the height of the internal boundary layer, i.e., for $z = 0$ to z_1 (or δ_i). Note that the wind shear data for all these cases is given in Appendix IV for convenience's sake. Subsequently, the momentum thickness was made dimensionless by referring it to the corresponding thickness of the internal boundary layer δ_i, i.e., θ/δ_i, where δ_i is, as previously indicated, denoted by z_1 in Tables 5, 6, and 7.

Variation of the dimensionless momentum thickness with the power-law index for these eleven cases is shown in Fig. 5.1 in order to compare it with that predicted by Eq. (5.2). Each case is identified by its reference number in this figure. An increase in the dimensionless momentum thickness with increasing power-law strikingly resembling that indicated by Eq. (5.2) is observed. The momentum thickness is consistently smaller for any power-law index than its counterpart given by Eq. (5.2), and the difference between them becomes greater as the power-law index increases. For instance, this difference increases from about 6% to 10% as the power-law index increases from 0.20 to 0.60. Examination of the variation of the dimensionless momentum thickness further reveals that it can be approximated by a relationship similar to Eq. (5.2) when the constant multiplying the power-law index in the denominator is 2.43, i.e., by the relation

$$\theta/\delta_i = \frac{\alpha}{(\alpha + 1)(2.43\alpha + 1)} \quad . \qquad (5.3)$$

Then the maximum power-law index, which corresponds to the largest dimensionless momentum thickness, is 0.642 since it is given by $(1/2.43)^2$. This maximum power-law index is about 9% smaller than that predicted by Eq. (5.2) (viz., 0.642 vs. 0.707) and is roughly 7% larger than its value indicated by the variation of the power-law index with increasing height of roughness element and/or roughness length (viz., 0.642 vs. 0.60). These results clearly indicate that the power-law index generally increases with increasing height of

roughness elements, with larger roughness length, and with greater dimensionless momentum thickness up to a certain maximum value. The existence of an upper bound in the value of the power-law index is of prime significance with regard to high surface roughness since it indicates that its value is not affected by further increase in the height of such roughness elements.

5.5 Correlation Between Power-Law Index and Roughness-Wind Interaction Parameter

Thus far, the effect of increasing height of roughness elements upon the power-law index was inspected. The height itself, notwithstanding its major importance, is only one of the characteristic geometric scales of a surface roughness. Moreover, the height is not related to the distribution of the roughness elements which affects significantly the wind shear and, hence, the power-law index. The other two characteristic length scales of the architecture of a surface roughness are the pitch and mesh of the roughness elements, which are shown in Fig. 4.1. In fact, the distribution of the roughness elements is determined by these two length scales. In order to account at once for all the three characteristic length scales and for the distribution of roughness elements, a surface-roughness structure index λ was advanced in Sect. 4.1. This structure index, which is approximated by the product of the ratios of height to pitch and height to mesh for three-dimensional roughness elements or only by the first ratio (height to pitch) for two-dimensional roughness elements (see Eqs. (4.3) and (4.4)), represents all the main features of the surface-roughness architecture. It is, therefore, important to examine how the power-law index changes with increasing structure index.

The variation of the power-law index α with increasing surface-roughness structure index λ, based on the data for very fine, fine, and high surface roughness compiled in Tables 5, 6, and 7, respectively, is shown in Fig. 5.7. Each case is denoted in this figure by its reference number. One can clearly discern a consistent increase in the power-law index with larger structure index up to a maximum value of 0.60 despite the inherent associated scattering. The power-law index attains its upper bound starting from a structure index of roughly 10. It is important to observe that the scattering in the results is particularly associated with cases 22, 51, 52, 56/a, 56/b, and 58/a. This scattering is, in all likelihood, a result of the various approximations used in estimating the pitch (and mesh) by means of the equivalent ideal surface roughness. The increasing pattern and, particularly, the existence of a maximum value of 0.60 are essentially similar to those found with higher height of the roughness elements (see Fig. 5.5). On the other hand, the rate of increase of the power-law index with larger structure index is much steeper than that with higher height except as its maximum value is approached. This steeper gradient can be attributed to the

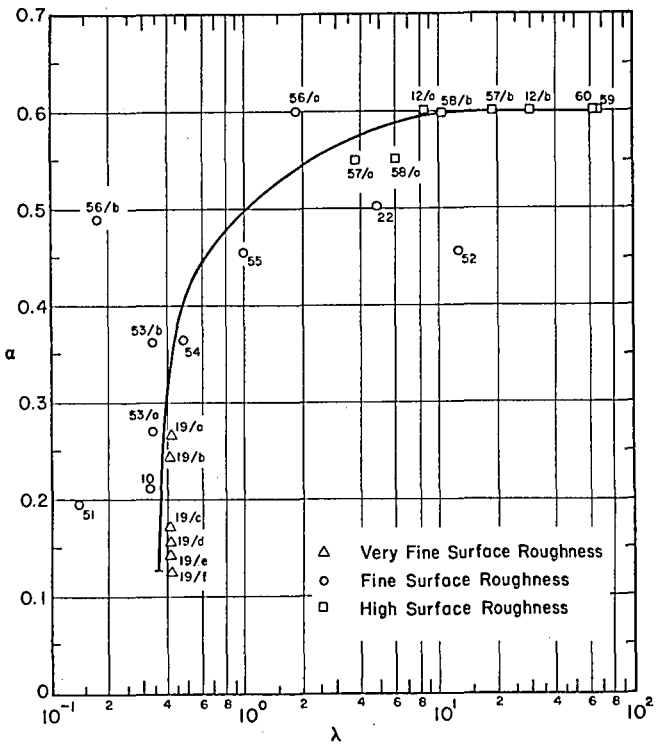

Figure 5.7.--Variation of the power-law index with increasing surface-roughness structure index.

effect of the pitch (and mesh) and, hence to the effect of the distribution of roughness elements.

In examining the dependence of the power-law index upon the structure index, the effect of the prevailing wind conditions is not accounted for. The structure index is, as a matter of fact, a geometric (or static) parameter which characterizes the surface-roughness architecture independently of the existing wind conditions. At the same time, the power-law index in flow above a surface roughness of a given structure index is affected, to a decisive extent, by the wind conditions. A reference-wind Reynolds number, based on the reference wind of the power law and the surface-roughness height, was introduced in Sect. 4.3 (see Eq. (4.5)) to describe the wind conditions in terms of a single characteristic parameter. It is thus relevant to inspect how the power-law index varies with increasing reference-wind Reynolds number.

The variation of the power-law index α with increasing reference-wind Reynolds number Re according to the results for very fine, fine, and high surface roughness tabulated in Tables 5, 6, and 7, respectively, is depicted in Fig. 5.8. Each case is designated in this figure, as commonly done, by its reference number. A continuous increase in the power-law index up to the same maximum value of 0.60 is readily discerned. This maximum value of the power-law index is reached starting from a Reynolds number of about 6×10^5. The scattering is almost minimal except

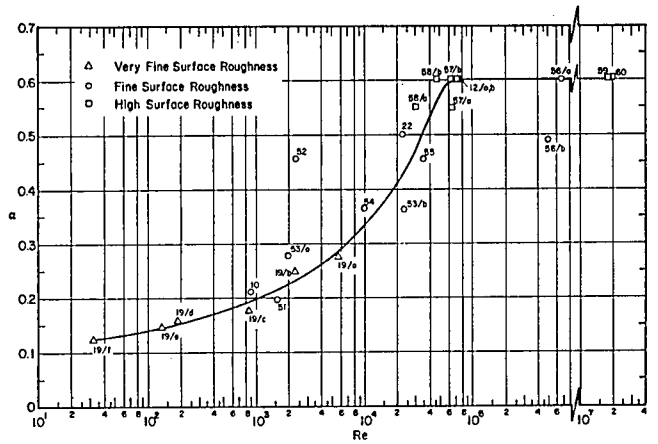

Figure 5.8.--Variation of the power-law index with increasing reference-wind Reynolds number.

for cases 52 and 56/b. It is further interesting to notice that the rate of increase of the power-law index with Reynolds number is much smaller than that with the structure index.

The power-law index exhibits a similar increasing behavior with larger structure index and higher Reynolds number. On the other hand, its rate of increase with these two parameters is significantly different. This indicates that the joint effect of these two parameters is to be considered. To this end, the roughness-wind interaction parameter was advanced in Sect. 4.4. This parameter, which is approximated by the product of the structure index and the Reynolds number according to Eqs. (4.6) or (4.7) for three- or two-dimensional roughness elements, respectively, accounts at once for the role of the surface-roughness architecture and the effect of the wind conditions.

The variation of the power-law index with increasing roughness-wind interaction parameter λRe, based on the results for very fine, fine, and high surface roughness given in Tables 5, 6, and 7, respectively, is portrayed in Fig. 5.9. As previously, each case is designated in this figure by its reference number. A strikingly continuous increase in the power-law index up to

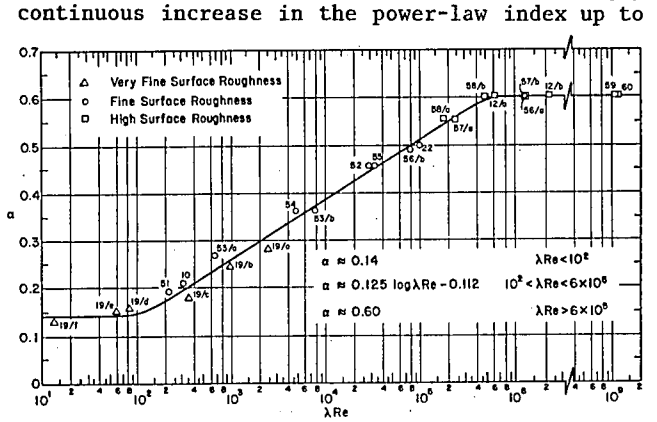

Figure 5.9.--Variation of the power-law index with increasing roughness-wind interaction parameter, i.e., power-law index--roughness-wind interaction parameter correlation.

its maximum value of 0.60 is observed. This continuous increase is fairly smooth, and it is not accompanied by any significant scattering as found for the structure index and/or the Reynolds number. The power-law index attains its constant maximum value starting from an interaction parameter of about $6x10^5$.

The continuous and smooth increase in the power-law index with larger interaction parameter is consequent upon the intrinsic nature of this parameter, which balances off the effects of the structure index and the Reynolds number. Comparison of the variation of the power-law index with the interaction parameter (see Fig. 5.9) to those with the structure index (see Fig. 5.7) and the Reynolds number (see Fig. 5.8) points out such a balancing role for the interaction parameter. It is, however, important to remark that the Reynolds number is the dominating factor in determining the value of the interaction parameter since it is generally greater than the structure index by several orders of magnitude. Inspection of the data given in Tables 5, 6, and 7 reveals, for instance, that the Reynolds number is larger than the structure index by two to six orders of magnitude, depending upon the prevailing wind conditions and the particular surface-roughness architecture. On the other hand, it is apparent that the rate of increase of the power-law index with increasing interaction parameter is affected by the structure index despite its relatively small value. This effect is consequent upon the steep gradient of the power-law index with increasing structure index.

The change in the power-law index with increasing interaction parameter approximated by a full line in Fig. 5.9 can be viewed as representative of an empirical correlation between these two variables. One can furthermore consider this correlation as being of universal nature since it encompasses all types of surface roughness and includes any prevailing wind conditions. Examination of this universal empirical correlation reveals that the power-law index: (1) is roughly constant and equal to 0.14 for any interaction parameter $\lambda Re < 10^2$; (2) exhibits a continuous increase at constant rate with increasing interaction parameter from 10^2 to $6x10^5$; and (3) takes on a constant maximum value of 0.60 for any interaction parameter $\lambda Re > 6x10^5$. It is, therefore, apparent that one can piecewise approximate the variation of the power-law index with increasing roughness-wind interaction parameter by the following three relationships:

$$\alpha \cong 0.14 \quad \text{for} \quad \lambda Re < 10^2 , \qquad (5.4a)$$

$$\alpha \cong 0.125 \ell og \lambda Re - 0.112 \quad \text{for} \quad 10^2 < \lambda Re < 6x10^5, \qquad (5.4b)$$

and

$$\alpha \cong 0.60 \quad \text{for} \quad \lambda Re > 6x10^5 . \qquad (5.4c)$$

It is important to recall that this universal correlation applies under thermally neutral conditions.

Comparison of the values of the power-law index approximated by the foregoing three relationships with their computed counterparts given in Tables 5, 6, and 7 indicates a reasonable agreement. They differ by 1% to, at most, 7% in most cases. For very large interaction parameters, which correspond to very high surface roughness, they are the same (0.60). Differences of 11% to 16% were found only in four isolated cases, viz., 19/a, 19/c, 19/d, and 53/a. This overall satisfactory agreement attests to the reliability of this universal correlation between the power-law index and interaction parameter as expressed by Eqs. (5.4).

It is apparent that Eqs. (5.4) supply a practical and expedient method for determining the power-law index in flow above any given surface roughness and for any wind conditions. Essentially, estimation of the power-law index depends, according to this universal correlation, upon knowing the roughness-wind interaction parameter. This parameter can be approximated for any surface roughness-wind situation since both the surface-roughness structure index and the reference-wind Reynolds number can readily be obtained. In order to compute the structure index, knowledge of the basic geometric characteristic scales of the surface roughness or of its equivalent ideal surface roughness--viz., height, pitch, and mesh--is needed. These three scales can easily be measured or estimated. Computation of the Reynolds number is contingent upon knowing the height of the surface roughness and the reference wind of the power law. The former is, at this point, known as a result of the estimation of the structure index. On the other hand, the reference wind is not known beforehand since it is the wind at the reference height of the power law. The latter is the thickness of the fully developed internal boundary layer, which can be evaluated as outlined in Sect. 4.1, and, therefore, the reference wind can readily be measured. In fact, this is the only flow property that is to be measured in order to compute the Reynolds number and, hence, the interaction parameter.

Computation of the interaction parameter entails evaluation of the reference height and wind scales of the power law. As a result, all three parameters of the power law--i.e., the power-law index, reference height, and reference wind--are obtained at once. Knowledge of these three parameters permits one to immediately describe and/or predict the wind shear above any surface roughness by means of a power law.

6. SUMMARY AND CONCLUSIONS

The main goal of this work was the development of a method for the estimation of the power-law index (or exponent) in flow above surface roughness ranging from very fine to high which entails specification of the similarity (or standard reference) height and wind scales of the power law. Currently, the power law is widely applied in describing the wind shear in flow above a surface roughness under thermally neutral conditions in engineering applications and meteorological work. The main reason for this extensive use is that the power law, consequent upon its empirical nature, is free of the constant shear-stress layer condition characteristic of the logarithmic law. Additional attractive features of the power law are its remarkable simplicity, engineering reliability, and operational expediency. However, the use of the power law depends on specifying its index and similarity scales for each surface roughness and prevailing wind conditions. Knowledge of the power-law index is furthermore of prime importance since it indicates the effect of turbulence induced by the surface roughness upon the wind shear.

To date, empirical estimation of the power-law index based either on the standard 10 m height wind or on the roughness length of the surface roughness have been offered. It is apparent, on the other hand, that the power-law index depends upon both the prevailing wind conditions and the architecture of the surface roughness. To this end, a roughness-wind interaction parameter, which accounts for both the surface-roughness architecture and the wind conditions, was introduced in this work. Then the method advanced herein consists of a universal empirical correlation between the power-law index and this interaction parameter. In order to obtain this universal correlation, it was necessary: (1) to determine standard reference scales for the power law related to each given surface roughness; (2) to represent the architecture of each surface roughness in terms of a unique surface-roughness structure index; (3) to express the prevailing wind conditions by means of a characteristic reference-wind Reynolds number; and (4) to advance a relationship for the roughness-wind interaction parameter.

In specifying reference scales for the power law representative of the effect of the surface roughness upon the flow and which can readily be determined, neither the commonly used geostrophic height and wind, nor the more rarely employed standard 10-m height and wind can be utilized. The former reference scales are primarily deduced by extrapolation assuming a priori a power-law wind variation since their direct measurement is seldom feasible. As a result, wide disparities in the geostrophic height in flow above identical and/or different types of surface roughness are obtained. The latter reference scales are, on the other hand, restricted to flow above open-country roughness.

The major change in the wind shear with height, the production, and most of the dissipation of turbulence in flow above a surface roughness transpire within its internal boundary layer. Consequently, the thickness of the fully developed internal boundary layer and the wind there were put forward as the standard reference scales of the power law. Approximation of the depth of the fully developed internal boundary layer was achieved based on the commonly accepted streamwise power-law growth in the thickness of the internal boundary layer. Empirical

representative values of the constant and exponent of this power-law growth, along with the streamwise fetch over which the full development of the internal boundary layer is attained, were submitted for flow above fine and high surface roughness based on reported data. These two major classes of surface roughness were primarily determined based on the height of the roughness elements and further corroborated according to their roughness length. Knowledge of the depth of the fully developed internal boundary layer permits one to immediately measure the corresponding wind. A third class of very fine surface roughness was further introduced in order to consider flow through a rough pipe. In this case, the thickness of the fully developed turbulent boundary layer (i.e., the pipe radius) and the velocity there were taken as the similarity scales of the power law.

Specification of the surface-roughness architecture involves the height and distribution of the roughness elements. The latter is determined by the pitch (axial spacing) and mesh (transverse spacing) of the roughness elements. These three characteristic length scales are not appropriately included in the currently used volumetric density number, roughness density, or roughness concentration indexes. In order to account for these three length scales, a surface-roughness structure index defined by the product of the ratios of height to pitch and height to mesh for three-dimensional roughness elements or by the ratio of height to pitch for two-dimensional roughness elements was introduced. This structure index applies to roughness elements of regular shape uniformly distributed. Any surface roughness consisting of roughness elements of irregular shape nonuniformly distributed can be modeled by an equivalent ideal surface roughness composed of identical rigid square prisms uniformly distributed. Such ideal roughness elements preserve the essential sharp corner separation characteristic of most natural and man-made roughness elements. These ideal elements are obtained under the condition that their height and volume, and their distribution are equal to those of the real irregular elements.

Description of the wind conditions above a given surface roughness by means of a single characteristic parameter was accomplished by advancing a Reynolds number based on the reference wind of the power law and the height of the surface roughness. Knowledge of the surface-roughness structure index and the reference-wind Reynolds number naturally led to expressing the roughness-wind interaction parameter in terms of their product.

The feasibility of the proposed method for the estimation of the power-law index was tested using wind-shear data reported in 24 representative cases of flow above very fine, fine, and high surface roughness. These 24 cases included six rough pipe flow, twelve wind-tunnel, and six field investigations. In each case, the standard reference scales of the power law, the surface-roughness structure index, the reference-wind Reynolds number, and the roughness-wind interaction parameter were computed. The latter three parameters exhibited increasing values with higher surface roughness notwithstanding some inherently associated scattering due to the random changes in the factors used in evaluating them.

Estimation of the power-law index was executed in each case by fitting a power-law variation to the reported wind-shear data, employing the corresponding reference height and wind. A similar increasing pattern in the power-law index with higher surface-roughness height, roughness length, structure index, reference-wind Reynolds number, and interaction parameter was found despite a certain degree of inevitable scattering. Consistently, the power-law index reached asymptotically a maximum value of about 0.60 in flow above high surface roughness. The existence of an upper bound in the value of the power-law index is in agreement with its variation according to the change in the momentum thickness within the internal boundary layer.

The change in the power-law index with increasing interaction parameter is viewed as being representative of a universal empirical correlation between these two variables. Such an interpretation is warranted since the entire range of values that the power-law index can take on (viz., roughly 0.14 to 0.60) all types of surface (viz., very fine, fine, and high) and any prevailing wind conditions are encompassed by this correlation. Based on inspection of this universal correlation, the power-law index was approximated piecewise by means of three relationships for interaction parameters smaller than 10^2, ranging between 10^2 and 6×10^5, and greater than 6×10^5, respectively. Then one can readily estimate the power-law index for any given interaction parameter.

In conclusion, computation of the roughness-wind interaction parameter necessarily involves evaluation of the reference scales of the power law. As a result, all three parameter, of the power law--viz., the power-law index, reference height and reference wind--are simultaneously obtained. Knowledge of these three parameters permits one to immediately describe and/or predict the wind shear above any surface roughness by means of a power law.

REFERENCES

1. Munn, R. E., Descriptive Micrometeorology, Academic Press Inc., New York, NY, 1966, pp. 56-59.

2. Sadeh, W. Z. and Cermak, J. E., "Simulation of Roughness Effects on Atmospheric Flow," Recent Advances in Engineering Science, Vol. 8, Pt. 3, ed. Chang, T. S., Proceedings, 10th Anniversary Meeting of the Society of Engineering Science, North Carolina State University, Raleigh, NC, 5-7 November 1973, Scientific Publishers, Inc., Boston, MA, 1977, pp. 309-318.

3. Sadeh, W. Z., "Role of Physical Modeling of Forest Canopy Flow in Forest Meteorology," Proceedings, Symposium on Forest Meteorology, World Meteorological Organization, University of Ottawa, Ottawa, Ontario, Canada, 21-25 August 1978, WMO-No. 527, Published on behalf of the WMO by the Canadian Forestry Service, 1979, pp. 45-50.

4. Sutton, O. G., Micrometeorology, McGraw-Hill Book Co., New York, NY, 1953, pp. 14-15; 82-85; 156; 238-241.

5. Lettau, H. H., "Theoretical Wind Spirals in the Boundary Layer of a Barotropic Atmosphere," Beitrage zur Physik der Atmosphaere (Contribution to Atmospheric Physics), Vol. 35, 1962, pp. 195-212.

6. Counihan, J., "Adiabatic Atmospheric Boundary Layers: A Review and Analysis of Data from the Period 1880-1972," Atmospheric Environment, Vol. 9, No. 10, October 1975, pp. 871-905.

7. Deland, R. J. and Binkowski, F. S., "Comparison of Wind at 500 ft Over Minneapolis and Louisville with Geostrophic Wind," Journal of the Air Pollution Association, Vol. 16, No. 8, 1966, pp. 407-411.

8. Lumley, L. J. and Panofsky, H. A., The Structure of Atmospheric Turbulence, Interscience Publishers, John Wiley & Sons, Inc., New York, NY, 1964, p. 100.

9. Elliot, W. P., "The Growth of the Atmospheric Internal Boundary Layer," Trans. American Geophysical Union, Vol. 39, No. 6, December 1958, pp. 1048-1054.

10. Antonia, R. A. and Luxton, R. E., "The Response of a Turbulent Boundary Layer to an Upstanding Step Change in Surface Roughness," Trans. ASME, Journal of Basic Engineering, Vol. 93, Series D, No. 1, March 1971, pp. 22-34.

11. Panofsky, H. A. and Townsend, A. A., "Change of Terrain Roughness and the Wind Profile," Quarterly Journal Royal Meteorological Society, Vol. 90, No. 384, April 1964, pp. 147-155.

12. Kawatani, T. and Sadeh, W. Z., "An Investigation of Flow Over High Roughness," TR CER71-72TK-WZS3, August 1971, Colorado State University, Fort Collins, CO.

13. Prandtl, L., "The Mechanics of Viscous Fluids," Division G, Aerodynamic Theory, ed. Durand, W. F., Vol. III, Dover Publications Inc., New York, NY, 1963, pp. 135-145.

14. Schlichting, H., Boundary Layer Theory, McGraw-Hill Book Co., Inc., New York, NY, 7th ed., 1979, pp. 141; 587-589; 599; 637.

15. Rossby, C. G. and Montgomery, R. B., "The Layers of Frictional Influence in Wind and Ocean Currents," Papers in Physical Oceanography and Meteorology, MIT and Woods Hole Oceanography Institution, Vol. 3, No. 3, 1935.

16. Sutton, O. G., Atmospheric Turbulence, Methuen Co. Ltd., London, 1949, pp. 55-57.

17. Deacon, E. L., "Vertical Profile of Mean Wind in the Surface Layers of the Atmosphere," Geophysical Memoirs, Vol. 11, No. 91, 1953.

18. Sadeh, W. Z., Cermak, J. E. and Kawatani, T., "Flow Over High Roughness Elements," Boundary Layer Meteorology, Vol. 1, No. 3, January 1971, pp. 321-344.

19. Nikurdase, J., "Laws of Flow in Rough Pipes," NACA TM 1292, 1950.

20. Thwaites, B., ed., Incompressible Aerodynamics, Oxford at the Clarendon Press, 1960, p. 57.

21. Frenzen, P., "The Observed Relation Between the Kolmogorov and von Kármán Constants in the Surface Boundary Layer," Boundary Layer Meteorology, Vol. 3, No. 3, February 1973, pp. 348-358.

22. Pasquill, F., "The Aerodynamic Drag of Grassland," Proceedings of the Royal Society A, Vol. 202, No. 1068, June 1950, pp. 143-153.

23. Wooding, R. A., Bradley, E. F., and Marshall, J. K., "Drag Due to Regular Arrays of Roughness Elements of Varying Geometry," Boundary-Layer Meteorology, Vol. 5, Nos. 1/2, April 1973, pp. 285-308.

24. Antonia, R. A., "Measurement of Reynolds Shear Stress Fluctuations in a Turbulent Boundary Layer," The Physics of Fluids, Vol. 15, No. 9, 1972, pp. 1669-1670.

25. Haugen, D. A., Kaimal, J. C. and Bradley, E. F., "An Experimental Study of Reynolds Stress and Heat Flux in the Atmospheric Surface Layer," Quarterly Journal Royal Meteorological Society, Vol. 97, No. 412, April 1971, pp. 168-180.

26. Lettau, H. H., "Note on Aerodynamic Roughness-Parameter Estimation on the Basis of Roughness-Element Description," Journal of Applied Meteorology, Vol. 8, No. 5, October 1969, pp. 828-832.

27. Plate, E. J. and Quaraishi, A. A., "Modeling of Velocity Distributions Inside and Above Tall Crops," Journal of Applied Meteorology, Vol. 4, No. 3, 1965, pp. 400-408.

28. Stevenson, T., "Report on the Simultaneous Observation of the Force of the Wind at Different Height Above the Ground," Journal of the Scottish Meteorological Society, Vol. 5, 1880, pp. 348-351.

29. Archibald, W., "An Account of Some Preliminary Experiments with Birams Anemometers Attached to Kite Strings," Nature, Vol. 31, 1885, p. 66.

30. De Marrais, G. A., "Wind-Speed Profiles at Brookhaven National Laboratory," Journal of Meteorology, Vol. 16, No. 2, April 1959, pp. 181-190.

31. Davenport, A. G., "Rationale for Determining Design Wind Velocities," Journal of the Structural Division, Proceedings ASCE, Vol. 86, No. ST5, May 1960, pp. 39-68.

32. Davenport, A. G., "The Relationship of Wind Structure to Wind Loading," Proceedings, Wind Effects on Buildings and Structures Conference, National Physical Laboratory, Teddington, Middlesex, 26-28 June 1963, Vol. 1, London: Her Majesty's Stationary Office, England, 1965, pp. 53-111.

33. Davenport, A. G., "The Dependence of Wind Loads on Meteorological Parameters," International Research Seminar Wind Effects on Buildings and Structures, Ottawa, Canada, 11-15 September 1967, Paper No. 2, University of Toronto Press, 1968, Toronto, Canada, pp. 19-82.

34. Hanna, R. S., "The Thickness of the Planetary Boundary Layer," Atmospheric Environment, Vol. 3, No. 5, September 1969, pp. 519-536.

35. Thuillier, R. H. and Lappe, U. O., "Wind and Temperature Profile Characteristics from Observation on a 1400 ft Tower," Journal of Applied Meteorology, Vol. 3, No. 3, June 1964, pp. 299-306.

36. Sherlock, R. H., "Variation of Wind Velocity and Gust with Height," Trans. ASME, Vol. 118, No. 2553, 1953, pp. 463-508.

37. Shellard, H. C., "Results of Some Recent Special Measurements in the United Kingdom Relevant to Wind Loading Problems," Proceedings, International Research Seminar, Wind Effects on Buildings and Structures, Ottawa, Canada, 11-15 September 1967, Vol. 1, University of Toronto Press, Toronto, Canada, 1968, pp. 515-533.

38. Pagon, W. W., "Wind Velocity in Relation to Height above Ground," Engineering News Record, Vol. 114, 1935, pp. 742-745.

39. Blackadar, A. K., "The Vertical Distribution of Wind and Turbulent Exchange in a Neutral Atmosphere," Journal of Geophysical Research, Vol. 67, No. 8, July 1962, pp. 3095-3102.

40. Deacon, E. L., "Gust Variation with Height up to 150 m," Quarterly Journal of the Royal Meterological Society, Vol. 81, 1955, pp. 562-573.

41. Collins, G. F., "Determining Basic Wind Loads," Proceedings ASCE, Structural Division, Vol. 81, Paper No. 825, November 1955, pp. 1-13.

42. Justus, C. G. and Mikhail, A., "Height Variation of Wind Speed and Wind Distribution Statistics," Geophysical Research Letters, Vol. 3, No. 5, May 1976, pp. 261-264.

43. Weibull, W., "A Statistical Distribution Function of Wide Applicability," Journal of Applied Mechanics, Vo. 18, No. 3, September 1951, pp. 293-297.

44. Peterson, E. W. and Hennessey, J. P., Jr., "On the Use of Power Laws for Estimates of Wind Power Potential," Journal of Applied Meteorology, Vol. 17, No. 3, March 1978, pp. 390-394.

45. Sadeh, W. Z., "Simulation of Flow above Forest Canopies," Proceedings, International Seminar on Heat and Mass Transfer in the Environment of Vegetation, Dubrovnik, Yugoslavia, 26-30 August 1974, eds. De Vries, D. A. and Afgan, N. H., Scripta Book Company, Washington, D.C., 1975, pp. 251-263.

46. Bettermann, D., "Contribution a l'Etude de la Couche Limite Turbulente le long de Plaques Rugueuses," Rapport 65-6, 1965, Centre National de le Recherche Scientifique, Paris, France.

47. Dvorak, F. A., "Calculation of Turbulent Boundary Layers on Rough Surfaces in Pressure Gradient," AIAA Journal, Vol. 7, No. 9, September 1969, pp. 1752-1759.

48. Schlichting, H., "Experimentelle Untersuchungen zum Rouhigkeits problem," Ing.-Arch., Vol. 7, 1936, (English Translation, Proc. ASME, 1936).

49. O'Loughlin, E. M.. "Flow Phenomena Near Rough Boundaries," Journal of Hydraulic Research, Vol. 7, No. 2, 1969, pp. 231-250.

50. Pretsch, J., "Zur theoretischen Berechnung des Profilwiderstandes," Jb. dtsch. Luftfahrtforsch., Vol. I, 1938, pp. 60-81.

51. Furuya, F., Miyata, M. and Fujita, H., "Turbulent Boundary Layer and Flow Resistance on Plates Roughened by Wires," Journal of Fluids Engineering, Vol. 98, Series 1, No. 4, December 1976, pp. 635-644.

52. Yeh, Fei-Fan and Nickerson, E. C., "Air Flow Over Roughness Discontinuity," TR CER70-71FFY-ECN6, July 1970, Colorado State University, Fort Collins, Colorado.

53. Moore, W. L., "An Experimental Investigation of the Boundary-Layer Development along a Rough Surface," Ph.D. Dissertation, Dept. of Mechanics and Hydraulics, Graduate College, State University of Iowa, Iowa City, Iowa, August 1951.

54. Mulhearn, P. J. and Finnigan, J. J., "Turbulent Flow Over a Very Rough, Random Surface," Boundary-Layer Meteorology, Vol. 15, No. 1, August 1978, pp. 109-132.

55. Blackadar, A. K., Panofsky, H. A., Glass, P. E. and Boogaard, J. F., "Determination of the Effect of Roughness Change on the Wind Profile," The Physics of Fluids Supplement, Vol. 10, Part II, No. 9, September 1967, pp. S209-S211.

56. Carl, D. M., Tarbell, T. C. and Panofsky, H. A., "Profiles of Wind and Temperature from Towers over Homogeneous Terrain," Journal of the Atmospheric Sciences, Vol. 30, No. 5, July 1973, pp. 788-794.

57. Kawatani, T. and Meroney, R. N., "The Structure of Canopy Flow Field," TR CER67-68TK66, August 1968, Colorado State University, Fort Collins, Colorado.

58. Ito, S., "Inner and Outer Flow Velocity Distributions Through Tall Simulated Vegetation," TR CER67-68JEC61, April 1968, Colorado State University, Fort Collins, Colorado.

59. "Diffusion under a Jungle Canopy," Final Report, February 1968, Meteorological Research Laboratory, Melpar, Inc., Falls Church, Virginia.

60. Shinn, J. H., "Steady-State Two-Dimensional Air Flow in Forests and the Disturbance of Surface Layer Flow by a Forest Wall," TR ECOM-5383, Atmospheric Sciences Laboratory, White Sands Missile Range, New Mexico, May 1971.

61. Fichtl, G. H. and McVehil, G. E., "Longitudinal and Lateral Spectra of Turbulence in the Atmospheric Boundary Layer at the Kennedy Space Center," Journal of Applied Meteorology, Vol. 9, No.1, February 1970, pp. 51-63.

APPENDIX I

DERIVATION OF EQUATION (3.2)

A set of continuously increasing average reference winds at 10 m height U_{10} (5 min average) from 4.47 to 31.29 m/s (10 to 70 mph) along with corresponding power-law indexes α were tabulated by Collins [41, p. 2]. The values of the power-law indexes were apparently obtained by fitting the power law to measured data. However, no information concerning the wind data, the surface roughness, and how the power-law index was estimated is given in this reference. The 10-m height reference winds and the power-law indexes reported by Collins are given in the table below:

U_{10} (m/s)	U_{10} (mph)	α
4.47	10	0.19
8.94	20	0.21
13.41	30	0.23
17.88	40	0.25
22.35	50	0.27
26.82	60	0.29
31.29	70	0.31

Examination of these data reveals that the power-law index varies linearly with the 10 m height reference wind according to the relation

$$\alpha = 0.0046U_{10} + 0.17, \qquad \text{(A.I.1)}$$

which is Eq. (3.2) in Sect. 3.2.

APPENDIX II

DERIVATION OF EQUATION (3.4)

Variation of the power-law index α with increasing roughness length z_0 is presented in the form of a graphical nomogram by Davenport [32, Fig. 3, p. 86]. This nomogram was compiled based on field data collected at more than 19 sites varying in their surface roughness from open sea to urban area. Examination of the graphical nomogram revealed that one can express the dependence of the power-law index upon the roughness length by means of the relationship

$$\alpha = 0.125\log z_0 + 0.0004/z_0 + 0.336, \qquad \text{(A.II.1)}$$

which is Eq. (3.4). This relationship, obtained by trial and error, used the values reported in the graphical nomogram over a roughness length range $z_0 = 0.01$ to 5.5 m (0.39 to 216.53 in). The values of the power-law index computed by means of the foregoing relationship are within -1.06% to +1.34% of their counterparts given in the subject nomogram.

APPENDIX III

PARAMETERS OF EQUATION (4.1)

The parameters of Eq. (4.1), which describes the growth of the thickness δ_i of the internal boundary layer with the streamwise distance x till its full development, are the exponent β and the constant C. Their characteristic values for flow over fine and high surface roughnesses were approximated using the wind-tunnel data reported by Antonia & Luxton [10] and Kawatani & Sadeh [12], respectively.

In Ref. 10 the growth of the internal boundary layer with the streamwise distance in flow over fine two-dimensional roughness (roughness element height h = 3.175 mm (1/8 in)) is approximated by a ½-power law, i.e., $\delta_i \sim x^{\frac{1}{2}}$. It is apparent that one can express the foregoing ½-power law growth of the internal boundary layer by $\delta_i = Ax^{\frac{1}{2}}$, where A is a constant whose value is to be determined. Examination of the data reported in Ref. 10 (Fig. 6, p. 25) revealed that $A \cong 0.25$ in. The data given in Ref. 10 was subsequently recast in terms of the roughness height h according to the form of Eq. (4.1), i.e., $\delta_i/h = C(x/h)^{\frac{1}{2}}$, where the constant $C = A/h^{\frac{1}{2}}$. Then the numerical value of the constant C is 0.707. Thus, it is proposed that $\beta = 0.5$ and $C = 0.707$ be applied for flow over fine surface roughness as indicated in Table 3.

The characteristic values of the exponent β and the constant C for flow over high surface roughness were approximated employing the wind-tunnel data in flow over a model forest canopy reported by Kawatani and Sadeh [12]. In this reference, the growth of the thickness δ_i of the internal boundary layer with the streamwise distance x is given in terms of δ_i/h vs. x/h [12, Fig. 5.31, p. 126], where h = 18 cm (7.1 in) is the height of the roughness elements (plastic trees). Data for the internal boundary layer over the streamwise distance corresponding to its full development (i.e., up to x/h 40) was replotted on logarithmic paper as displayed in Fig. A.III.1. Inspection of this plot reveals that the internal boundary layer grows up to its full development according to the power law given by Eq. (4.1) when $\beta = 0.466$ and $C = 1.16$. It is consequently suggested that these values be applied for flow over high surface roughness, as noted in Table 3.

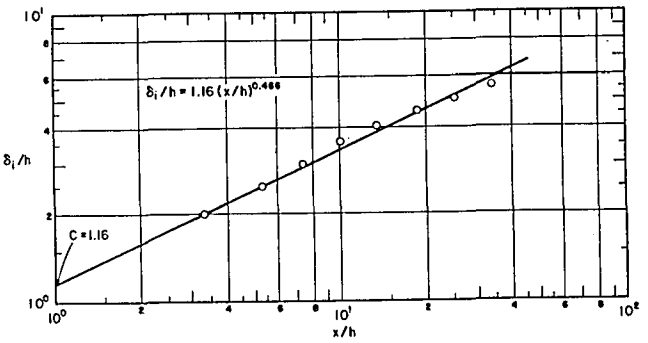

Figure A.III.1.--Internal boundary layer growth with increasing streamwise distance based on the data reported in Ref. 12.

APPENDIX IV

ESTIMATION OF PARAMETERS GIVEN IN TABLES 4, 5, 6, AND 7

A brief description of how the roughness length, the reference height and velocity, and the pitch and mesh were estimated from the data reported in the 24 investigations listed in Table 4 is given herein. These parameters are tabulated in Tables 4, 5, 6, and 7 for flow above very fine, fine, and high surface roughness, respectively. The roughness length was estimated by fitting a log law or a modified log law to the given wind shear data whenever it was not reported. Approximation of the standard reference height and wind of the power law was accomplished according to the method advanced in Sect. 4.1. Herein, the reference height of the power law, which is estimated by the height of the fully developed internal boundary layer, is denoted by z_1 as starting from Sect. 5.3 (and not by δ_1 as in Sect. 4.1) for consistency with the accepted notation. The pitch and mesh for roughness elements of regular geometric shape were determined based on the reported center-to-center (or edge-to-edge) spacing between the elements since they were uniformly distributed in all the cases. Any surface roughness consisting of three-dimensional roughness elements of irregular shape with sharp corners was represented by an ideal surface roughness composed of square prisms uniformly distributed, as outlined in Sect. 4.2 (see also Figs. 4.1 and 4.2). The sides and height of the equivalent ideal square prism were computed based on the conditions that its volume and height are equal to those of the real roughness element. Then the pitch and mesh were estimated in the same manner as for roughness elements of regular geometric shape. The sand grains used in the rough pipe flow study reported in Ref. 19 were modeled by identical spheres according to the suggestion advanced there. Note that the pitch is the only spacing of interest for two-dimensional roughness elements. Whenever three-dimensional roughness elements are uniformly distributed and of equal sides, their pitch and mesh are equal. The wind shear data for each case is further tabulated in Sect. IV.4.

IV.1 Very Fine Surface Roughness - Table 5

Source: Nikuradse [19], cases 19/a,19/b,19/c, 19/d,19/e, and 19/f.

Experimental environment: Water flow in a rough pipe.

Roughness elements: Sand grains of roughly spherical shape and of various diameters h randomly distributed (pp. 6-7; Fig. 4, p. 47).

Type of roughness elements: Three dimensional.

Velocity data used: Velocity measured at a streamwise distance larger than 1200h from the pipe inlet (p. 9). Data for six cases, denoted by 19/a to 19/f, which include two different maximum velocities for three different roughness heights, were used. The basic data for these six cases along with information where they are given in Ref. 19 are summarized in the table below:

Case	Table No. in Ref. 19	Page No. in Ref. 19	Pipe Radius R (cm)	Relative Roughness R/h	Roughness Height h (mm)	Maximum Velocity U_1 (cm/s)	P or M (mm)
19/a	13	42	1.206	15	0.8	707.0	1.20
19/b						286.5	
19/c	11	40	1.217	60	0.2	419.5	0.30
19/d						93.0	
19/e	8	37	4.970	507	0.098	141.4	0.147
19/f						33.0	

Note that the height of the sand grains (i.e., their diameter) is denoted by k in Ref. 19. The maximum velocity U_1 is the velocity measured along the pipe axis, which is given in the tables in Ref. 19 as the velocity at $y/R = 1$, where y designates the distance from the wall.

Roughness length z_0: Estimated by graphically fitting a log law according to Eq. (2.1) to the reported velocity data.

Reference height z_1: The thickness of the fully developed boundary layer, which is equal to the pipe radius R (measured from the wall) since it is the characteristic length for this pipe flow. It is given in the table above for all the six cases.

Reference wind U_1: Velocity along the pipe axis (at $y/R = 1$), which is the maximum velocity and which is tabulated in the table above.

Pitch and mesh: An average center-to-center spacing between two sand grains of about 2.5h was deduced from a still photograph (X20) of the surface roughness (h = 0.8 mm (31.5 mils)) given in Fig. 4 (p. 47) assuming that the sand grains were spheres of diameter h uniformly distributed. Then the pitch and the mesh are equal and given by

$$p = 2.5h - h = 1.5h. \qquad \text{(IV.1)}$$

Based on the description of the distribution of the sand grains, the same center-to-center spacing was assumed to apply to the other two sand grains heights (h = 0.098 and 0.2 mm (3.9 and 7.9 mils)). The pitch (or mesh) is given in the table above for all the six cases.

IV.2 Fine Surface Roughness - Table 6

Source: Furuya, Miyata, and Fujita [51].

Experimental environment: Wind tunnel.

Roughness elements: Wires of diameter h = 0.2 cm (0.079 in; denoted by k in Ref. 51) uniformly distributed with a center-to-center spacing of 8h (p. 636).

Type of roughness elements: Two dimensional.

Velocity data used: Velocity measured at a streamwise distance x/h = 95 (x = 19 cm (7.48 in)) given in Fig. 3 (p. 637) for a center-to-center spacing of 8h between two wires.

Roughness length z_0: Estimated by graphically fitting a log law according to Eq. (2.1) to the reported velocity data.

Reference height z_1: Estimated by means of Eq. (4.1), i.e., $z_1 = 6.707h = 1.34$ cm (0.53 in).

Reference wind U_1: Velocity at height z_1 obtained from the velocity data given in Fig. 3 (p. 637).

Pitch: Since the center-to-center spacing between two wires was 8h, the pitch is

$$P = 8h - h = 7h = 1.4 \text{ cm } (0.55 \text{ in}). \quad \text{(IV.2)}$$

Source: Antonia and Luxton [10].

Experimental environment: Wind tunnel.

Roughness elements: Square bars of height h = 0.3175 cm (1/8 in) uniformly distributed with a center-to-center spacing of 4h (Fig. 2, p. 24).

Type of roughness elements: Two dimensional.

Velocity data used: Velocity measured at a streamwise distance x/h = 120 (x = 38.1 cm (15 in)) given in Fig. 7 (p. 26) as the velocity at the position of element no. 31.

Roughness length z_0: Estimated by graphically fitting a log law according to Eq. (2.1) to the reported data.

Reference height z_1: Computed by means of Eq. (4.1), i.e., $z_1 = 6.707h = 2.13$ cm (0.84 in).

Reference wind U_1: Velocity at height z_1 obtained from the velocity data for element no. 31 given in Fig. 7 (p. 26).

Pitch: Since the center-to-center spacing between two bars was 4h, the pitch is:

$$P = 4h - h = 3h = 0.9525 \text{ cm } (0.38 \text{ in}). \quad \text{(IV.3)}$$

Source: Yeh and Nickerson [52].

Experimental environment: Wind tunnel.

Roughness elements: Gravel pieces of irregular shape with sharp corners and of roughly same height h = 0.635 cm (1/4 in) randomly distributed (p. 24).

Type of roughness elements: Three dimensional.

Velocity data used: Velocity measured at a streamwise distance x/h = 96 (x = 60.96 cm (24 in)) given in Table 1, case I (p. 67).

Roughness length z_0: Given at x = 60.96 cm (24 in) in Table IV, case I (p. 70).

Reference height z_1: Estimated by means of Eq. (4.1), i.e., $z_1 = 6.707h = 4.26$ cm (1.68 in).

Reference wind U_1: Velocity at height z_1 deduced from the given velocity data.

Pitch and mesh: Since the gravel pieces are generally small stones of irregular shape with sharp corners, they were modeled by ideal square prisms uniformly distributed. In Ref. 52 only the average height h of the gravel is given. In view of lack of information on the other dimensions of the gravel pieces, their average volume was approximated assuming that their average height is the diameter of a sphere, i.e., $V = (4\pi/3)(h/2)^3$. Then the height h and sides s of the equivalent ideal prism were computed based on the conditions that its volume and height are equal to those of the average sphere. Thus,

$$s^2h = (4\pi/3)(h/2)^3, \quad \text{(IV.4)}$$

and then

$$s = 0.7236h. \quad \text{(IV.5)}$$

The center-to-center spacing between two gravel pieces was roughly equal to the average height of the gravel (Fig. 1, p. 82). Consequently, the pitch and mesh of the ideal square prisms, which are equal, are given by

$$P = h - 0.7236h = 0.2764h$$

$$= 0.1755 \text{ cm } (0.069 \text{ in}). \quad \text{(IV.6)}$$

Source: Moore [53], cases 53/a and 53/b.

Experimental environment: Wind tunnel

Roughness elements: (1) Case 53/a: Square bars of height h = 0.3276 cm (0.129 in).

(2) Case 53/b: Square bars of height h = 3.89 cm (1.53 in). In both cases the square bars were uniformly distributed with an edge-to-edge spacing of about 3.9h (Fig. 3, p. 40).

Type of roughness elements: Two dimensional.

Velocity data used: Case 53/a: Velocity data at a streamwise distance x/h = 90 (29.5 cm (11.6 in)) obtained by interpolation of reported velocity data at x/h = 77.5 and 155 (29.1 and

50.8 cm (10 and 20 in)) given in Fig. 7 (p. 45; velocity 30.2 ft/s).

Case 53/b: Velocity data at x/h = 90 (x = 350 cm (137 in)) obtained by extrapolation employing reported velocity data at x/h = 57 and 76 (221 and 297 cm (87 and 117 in)) given in Fig. 9 (p. 47; velocity 29.7 ft/s).

Roughness length z_0: Case 53/a: Estimated by graphically fitting a log law to the velocity data according to Eq. (2.1).

Case 53/b: Estimated by graphically fitting a modified log law to the velocity data according to Eq. (2.2) (d = h).

Reference height z_1: Estimated by means of Eq. (4.1), i.e., $z_1 = 6.707h = 2.2$ and 26.1 cm (0.87 and 10.28 in) for cases a and b, respectively.

Reference wind U_1: Deduced in both cases from the velocity data at the corresponding reference heights.

Pitch: Since the edge-to-edge spacing between two bars was about 3.9h, the pitch is given by

$$P = 39h - h = 2.9h. \qquad \text{(IV.7)}$$

Thus, P = 0.95 and 11.3 cm (0.37 and 4.45 in) for cases a and b, respectively.

Source: Mulhearn [54].

Experimental environment: Wind tunnel.

Roughness elements: Gravel pieces of irregular shape with sharp corners randomly distributed, described as spheres of an average diameter h = 1.45 cm (0.57 in; p. 110).

Type of roughness elements: Three dimensional.

Velocity data used: Velocity measured at 91.3 cm (35.94 in) upstream of the downwind end of the surface roughness (Fig. 6, p. 115). This position corresponds to a streamwise distance x/h = 91 (x = 131.7 cm (51.85 in)) measured from the front end of the streamwise zero pressure gradient region since the length of this region was 223 cm (87.79 in; Fig. 1, p. 110).

Roughness length z_0: Given (p. 118).

Reference height z_1: Estimated according to Eq. (4.1), i.e., $z_1 = 6.707h = 9.73$ cm (3.83 in).

Reference wind U_1: Deduced from the reported velocity data at the corresponding reference height.

Pitch and mesh: The gravel pieces used were of irregular shape with sharp corners, as can be observed in the still photograph of the rough surface given in Fig. A3 (p. 129). Therefore, they were modeled by ideal square prisms uniformly distributed in a similar manner as for the gravel pieces reported in Ref. 52. Based on the given average number of stones per square meter (1017 stones/m^2, p. 110), the center-to-center spacing between two gravel pieces was approximated by $(1017 \text{ stones/m}^2)^{-\frac{1}{2}} = 3.14$ cm (1.24 in). Then the sides of the ideal square prism s = 0.7236h according to Eq. (IV.5) when its height h = 1.45 cm is taken equal to the diameter of the sphere used to approximate the height of the gravel. Consequently, the pitch and mesh of the equivalent surface roughness, which are equal, are given by the center-to-center spacing less the side of the ideal prism, i.e., by

$$P = 3.14 - 0.7236h = 2.09 \text{ cm (0.82 in)}. \qquad \text{(IV.8)}$$

Source: Pasquill [22].

Experimental environment: Field.

Roughness elements: Clayland pasture covered by randomly distributed grass of height h = 1 to 15 cm (0.39 to 5.91 in; p. 146).

Type of roughness elements: Three dimensional.

Wind data used: Wind data above grass of height h = 5 to 10 cm (1.97 to 3.94 in) for a wind of 513 cm/s (16.83 ft/s) at a height of 100 cm (39.37 in; measured from the ground) given in Table 1 (p. 147). It is conceivable to assume that the wind profile was measured at a streamwise distance x/h > 90 since the terrain was generally similar over a distance of, at least, 137.2 m (150 yd) upwind of the measurement site (p. 146).

Roughness length z_0: Given (p. 150).

Reference height z_1: Estimated by means of Eq. (4.1) based on an average grass height h = 7.5 cm (2.95 in), i.e., $z_1 = 6.707h = 50.30$ cm (19.80 in).

Reference wind U_1: Wind at height z_1 deduced from the reported wind data.

Pitch and mesh: No estimation of the pitch and mesh was readily feasible in view of the sketchy description of the grass cover. They were then approximated based on inspection of roughly similar grass covers. A pitch and an equal mesh of about 3.5 cm (1.38 in) were deduced for grass elements of an average height of 7.5 cm assuming uniform distribution. This pitch (and mesh) is highly conjectural but, nevertheless, it was used because of the lack of sufficient information.

Source: Blackadar, Panofsky, Glass, and Boogaard [55].

Experimental environment: Field.

Roughness elements: Unharvested hay of about a height h = 20 cm (7.87 in; p. S209).

Type of roughness elements: Three dimensional.

Wind data used: Wind data at a streamwise distance $x/h = 90$ (at $x = 18$ m (59.06 ft)) obtained by interpolation of measured wind at 6 and 30 m (19.69 and 98.43 ft) upwind and downwind, respectively, of the front end of the surface roughness, which are given in Fig. 2 (p. S210).

Roughness length z_0: Given (p. S209).

Reference height z_1: Estimated by means of Eq. (4.1), i.e., $z_1 = 0.6707h = 134.14$ cm (52.81 in), where $h = 20$ cm.

Reference wind U_1: Wind at height z_1 deduced from the wind data.

Pitch and mesh: No estimation of the pitch and mesh was readily feasible because of the sketchy description of the hay cover. They were approximated, as in the case of Ref. 22, based on inspection of roughly similar hay covers. Average pitch and mesh equal to the height of the hay elements were inferred assuming uniform distribution, i.e., P (or M) = 20 cm. In spite of the ambiguity of this pitch (and mesh) with regard to the given hay cover, it was employed in view of the lack of better information.

Source: Carl, Tarbell, and Panofsky [56], cases 56/a and 56/b.

Experimental environment: Field.

Roughness elements: (1) Case 56/a: Roughly uniform terrain covered with sagebrush (Arco, Idaho, p. 790). Since the height of the sagebrush elements is not given, an average height $h = 1$ m (3.28 ft) was assumed based on inspection of sagebrush covers.

(2) Case 56/b: Homogeneous flat terrain covered with low vegetation 1 to 2 m (3.28 to 6.56 ft) high, i.e., average height $h = 1.5$ m (4.92 ft; Cape Kennedy, p. 790; see also Ref. 61, p. 51).

Type of roughness elements: Three dimensional.

Wind data used: Cases 56/a and 56/b: Wind data given in Fig. 2 (p. 789) assuming that the measurement sites were located in both cases at a streamwise distance $x/h \geq 90$ ($x > 90$ and 135 m (295.2 and 442.8 ft) for cases a and b, respectively). This is a plausible assumption considering that meteorological towers were employed.

Roughness length z_0: Estimated in both cases by graphically fitting a modified log law according to Eq. (2.2) ($d = h$) to the reported wind data. The value of the roughness length obtained for case 56/b is smaller by 3% than its value given in Ref. 61 (p. 56).

Reference height z_1: Estimated by means of Eq. (4.1) based on average heights of 1 and 1.5 m for cases 56/a and 56/b, respectively, i.e., $z_1 = 6707h = 670.7$ and 1006 cm (22 and 33 ft).

Reference wind U_1: Wind at height z_1 deduced from the reported wind data in each case.

Pitch and mesh: Average pitches and meshes of about 0.75h (75 cm (29.52 in)) and 2.5h (375 cm (147.64 in)) were conjectured for cases 56/a and 56/b, respectively, assuming uniform distribution of the roughness elements. These estimates were deduced based on inspection of roughly similar surface roughnesses. They are highly conjectural but, nevertheless, they are used in view of the lack of sufficient information.

IV.3 High Surface Roughness - Table 7

Source: Kawatani and Meroney [57], cases 57/a and 57/b.

Experimental environment: Wind tunnel.

Roughness elements: Uniform pegs of a height $h = 9$ cm (3.54 in) and 0.48 cm (3/16 in) in diameter uniformly distributed in square arrays of 5.08 and 2.54 cm (2 and 1 in) in cases 57/a and 57/b, respectively (p. 20 and Fig. 2, p. 52).

Type of roughness elements: Three dimensional.

Velocity data used: (1) Case 57/a: Velocity measured at a streamwise distance $x/h = 33.33$ ($x = 3$ m (9.89 ft)) given in Table 4 (p. 108).

(2) Case 57/b: Velocity measured at a streamwise distance $x/h = 44.44$ ($x = 4$ m (13.12 ft)) given in Table 2 (p. 106).

Roughness length z_0: Estimated in each case by graphically fitting a modified log law according to Eq. (2.2) ($d = h$) to the reported velocity data. Roughness lengths 3.1 and 4.5 times larger are given in Ref. 57 (Fig. 16, p. 66) for cases 57/a and 57/b, respectively. These uncommonly high roughness lengths (viz., 10% and 38% of the height of the roughness elements) were apparently calculated by piecewise application and averaging of the modified log law.

Reference height z_1: Estimated in both cases by means of Eq. (4.1), i.e., $z_1 = 6.081h = 55$ cm (21.65 in). Slightly different heights of the internal boundary layer (viz., the reference height z_1) are given in Ref. 57 (Figs. 30 and 31, pp. 80-81). They were estimated based on different criteria than those used in this work.

Reference wind U_1: Deduced in both cases from the velocity data at the corresponding reference heights.

Pitch and mesh: Since the peg diameter (0.48 cm) and the center-to-center spacing between the two pegs in both streamwise and transverse directions are known (5.08 and 2.54 cm square array), the pitch and the mesh, which are equal, are given by the center-to-center spacing less the peg diameter, as tabulated in the table below:

Case	Center-to-Center Spacing (cm)	Pitch (or Mesh) (cm)
57/a	5.08	4.60
57/b	2.54	2.06

Source: Ito [58], cases 58/a and 58/b.

Experimental environment: Wind tunnel.

Roughness elements: (1) Case 58/a: Uniform pegs of a height h = 5.08 cm (2 in) and 0.48 cm (3/16 in) in diameter uniformly distributed in a 2.54 cm (1 in) square array (p. 3 and Fig. 2-2, p. 31).

(2) Case 58/b: Rectangular flexible plastic strips of a height h = 10.16 cm (4 in), 0.635 cm (1/4 in) wide and 0.019 cm (7.5 miles) thick, uniformly distributed in a 5.08x2.54 cm (2x1 in; row-to-row streamwise spacing x center-to-center transverse spacing between two elements) rectangular array (p. 3 and Fig. 2-1, p. 31).

Type of roughness elements: Three dimensional.

Velocity data used: (1) Case 58/a: Velocity measured at x/h = 42 (x = 213.4 cm (84 in)) given in Fig. 4-5 (p. 44).

(2) Case 58/b: Velocity data at x/h = 35 (x = 355 cm (140 in)) obtained by interpolation of velocity measured at x/h = 30 (x = 304.8 cm (120 in)) and 54 (x = 548.6 cm (216 in)) given in Fig. 4-4 (p. 43).

Roughness length z_0: Estimated in each case by graphically fitting a modified log law according to Eq. (2.2) (d = h) to the velocity data. Roughness lengths larger by about 45% and 6% are reported in Ref. 58 (Figs. 4-5 and 4-4). They were obtained based on the log law and not on the modified log law.

Reference height z_1: Estimated in both cases by means of Eq. (4.1), i.e., $z_1 = 6.081h = 31$ and 62 cm (12.20 and 24.41 in) for cases a and b, respectively.

Reference wind U_1: Deduced in both cases from the velocity data at the corresponding reference heights.

Pitch and mesh: (1) Case 58/a: They are given by the center-to-center spacing (2.54 cm) less the peg diameter (0.48 cm), as in case 57/b. Thus, P (or M) = 2.06 cm (0.81 in).

(2) Case 58/b: The pitch is given by the row-to-row streamwise spacing, i.e., P = 5.08 cm (2 in), while the mesh is given by the transverse center-to-center spacing between two elements less the strip width, i.e., M = 1.9 cm (0.75 in).

Source: Kawatani and Sadeh [12] cases 12/a and 12/b.

Experimental environment: Wind tunnel.

Roughness elements: Plastic model trees of a height h = 18 cm (7.09 in) randomly distributed (p. 16).

Type of roughness elements: Three dimensional.

Velocity data used: Velocity measured at x/h = 38.88 (x = 7 m (22.97 ft)) given in Table 1-HDC (Half-density canopy-HDC, p. 145) and Table 1-FDC (Full-density canopy-FDC, p. 144) for cases 12/a and 12/b, respectively.

Roughness length z_0: Estimated by graphically fitting a modified log law according to Eq. (2.2) (d = h) to the velocity data for each of the two cases.

Reference height z_1: Estimated by means of Eq. (4.1), i.e., $z_1 = 6.081h = 109$ cm (42.91 in) for both cases. This estimated height is about 9% and 3.8% greater than the height of the internal boundary layer for FDC and HDC reported in Ref. 12. These slight differences can be attributed to the approximations involved in obtaining Eq. (4.1) (see Appendix III).

Reference wind U_1: Deduced in both cases from the velocity data at the corresponding reference heights.

Pitch and mesh: The tree elements were modeled by ideal square prisms uniformly distributed in view of their irregular shape. To this end, each tree element was first represented, as suggested in Ref. 12 (p. 17 and Fig. 3.1, p. 85), by: (1) a cylindrical trunk of diameter d_t = 0.5 cm (0.20 in) and height h_t = 5 cm (1.97 in); and (2) a conical crown of a base diameter d_c = 8 cm (3.15 in) and height h_c = 13 cm (5.12 in). The height h and sides s of the equivalent ideal square prisms were computed based on the conditions that its volume and height are equal to those of the tree element. Thus,

$$\pi(d_t^2/4)h_t + (\pi/3)(d_c^2/4)h_c = s^2h, \qquad \text{(IV.9)}$$

in which h = 18 cm and, therefore, s = 3.5 cm (1.38 in). Based on the given densities of the tree elements (pp. 16-17)--viz., 1 tree/92 cm^2 and 1 tree/46 cm^2 in cases 12/a (HDC) and 12/b (FDC), respectively--the average center-to-center spacings in the two cases are given by 92 cm^2/1 tree and 46 cm^2/1 tree. Then the pitch and mesh, which are equal in view of the assumed uniform distribution, are approximated by the difference between the center-to-center spacing and the side of the ideal square prism. Their values for the two cases are given in the table below:

Case	Density of Tree Elements	Center-to-Center Spacing (average) (cm)	Pitch (or Mesh) (cm)
12/a (HDC)	1 tree/92 cm^2	9.6	6.1
12/b (FDC)	1 tree/46 cm^2	6.8	3.3

Source: Diffusion Under Jungle Canopy [59].

Experimental environment: Field.

Roughness elements: Dominant trees of height h = 30 m (98.43 ft) non-uniformly distributed (Vol. I, p. 7 and Fig. 8, p. 13).

Type of roughness elements: Three dimensional.

Wind data used: Wind measured under most nearly neutral conditions (trial 11) given in Fig. 35 (Vol. I, p. 81). It is apparent, based on the site map (Vol. I, Fig. 3, p. 8), that the meteorological tower was located at a streamwise distance $x/h > 35$ ($x > 1050$ m (3444 ft)).

Roughness length: Given (Vol. I, p. 80).

Reference height z_1: Estimated by means of Eq. (4.1), i.e., $z_1 = 6.081h = 182.4$ m (598 ft).

Reference wind U_1: Wind at height z_1 estimated by extrapolation of the wind data which were given up to a height of about $z_1/3$.

Pitch and mesh: Approximated by the overall mean spacing between dominant trees of mode of height h = 30 m (100 ft) given in Table 30 (Vol. II, p. 135), assuming uniform distribution, i.e., P (or M) = 3.75 m (12.3 ft). In using this pitch (and mesh) it was tacitly assumed that the same mean spacing would be effective if the trees were represented by their equivalent ideal square prisms uniformly distributed.

Source: Shinn [60].

Experimental environment: Field.

Roughness elements: Gum-maple trees of height h = 31 m (101.71 ft), randomly distributed (Table II, p. 12 and Fig. A-4, p. 72).

Type of roughness elements: Three dimensional.

Wind data used: Wind measured inside and above a gum-maple forest given in Table V (p. 23). The meteorological tower was located more than 3 km (1.86 mi) from the nearest forest wall (p. 70), i.e., at a streamwise distance $x/h > 35$.

Roughness length: Given in Table II (p. 12).

Reference height z_1: Estimated by means of Eq. (4.1), i.e., $z_1 = 6.081h = 188.5$ m (618 ft).

Reference wind U_1: Wind at height z_1 estimated by extrapolation of the reported wind data, which were given up to the height of about $z_1/3$.

Pitch and mesh: Based on the given distribution of the tree elements of 264 trees per acre (p. 70), the pitch and the mesh were approximated by the average spacing between the trees $(4047\ m^2/264\ \text{trees})^{\frac{1}{2}}$, assuming uniform distribution, i.e., P (or M) = 3.9 m (12.80 ft). In using this pitch (and mesh) it was assumed, as for Ref. 59, that the trees are represented by their equivalent ideal square prisms.

TABLE A.IV.1. WIND-SHEAR DATA FOR VERY FINE SURFACE ROUGHNESS

Source:	Nikuradse								
Ref. No.		19/a	19/b		19/c	19/d		19/e	19/f
Page/Fig. or Table		42/13	42/13		40/11	40/11		37/8	37/8
	z (mm)	U (cm/s)	U (cm/s)	z (mm)	U (cm/s)	U (cm/s)	z (mm)	U (cm/s)	U (cm/s)
	0.240	270.0	107.0	0.24	211.0	50.6	0.99	84.0	19.0
	0.480	320.0	136.0	0.85	277.0	62.5	3.48	101.3	23.0
	0.845	367.0	158.0	1.83	314.0	71.0	7.50	112.0	25.8
	1.200	406.0	174.0	3.65	352.0	79.0	14.91	123.0	28.3
	2.400	492.0	206.0	6.08	381.0	85.0	24.85	132.0	30.4
	4.830	585.0	243.0	8.52	402.0	89.0	34.80	137.6	31.8
	7.240	647.0	263.0	10.95	416.0	92.2	44.73	140.8	32.8
	10.850	701.0	283.0	12.17	419.5	93.0	49.70	141.4	33.0
	12.060	707.0	286.5						

TABLE A.IV.2. WIND-SHEAR DATA FOR FINE SURFACE ROUGHNESS

Source:	Furuya et al.		Antonia & Luxton		Yeh & Nickerson		Mulhearn	
Ref. No.	51		10		52		54	
Page/Fig. or Table	637/3		26/7		67/1		115/6	
	z (mm)	U (cm/s)	z (mm)	U (cm/s)	z (mm)	U (cm/s)	z (mm)	U (cm/s)
	2.00	840.0	4.06	244.0	9.50	240.8	15.0	427.7
	4.00	913.5	7.70	335.0	11.00	265.2	20.0	500.0
	6.00	1023.8	12.45	366.0	19.00	368.8	30.0	677.7
	8.00	1102.5	16.30	396.2	25.40	420.0	40.0	755.5
	10.00	1128.8	21.30	425.0	31.75	457.2	50.0	850.0
	12.00	1155.0			35.00	510.5	65.0	911.1
	13.40	1195.0			42.60	533.0	97.2	1033.0

Source:	Moore				Pasquill		Blackadar et al.	
Ref. No.	53/a		53/b		22		55	
Page/Fig. or Table	45/7		47/9		147/1		S210/2	
	z (mm)	U (cm/s)	z (cm)	U (cm/s)	z (cm)	U (cm/s)	z (cm)	U (cm/s)
	4.4	624.8	6.4	588.4	25.0	347.8	20.0	100.0
	6.6	725.4	9.6	688.0	37.5	381.0	40.0	126.4
	8.8	792.5	12.8	769.3	50.3	437.0	60.0	150.0
	13.2	899.1	19.2	887.1			80.0	171.4
	22.0	920.0	26.1	905.0			100.0	205.0
							120.0	235.3
							134.1	253.0

Source:	Carl et al.		
Ref. No.	56/a	56/b	
Page/Fig. or Table	789/2	789/2	
	z (cm)	z (cm)	U (cm/s)
	200.0	500	200	240
	250.0	575	300	310
	300.0	650	400	360
	400.0	775	500	395
	500.0	885	600	425
	670.7	1000	700	450
			900	480
			1006	500

TABLE A.VI.3. WIND-SHEAR DATA FOR HIGH SURFACE ROUGHNESS

Source:	Kawatani & Meroney		Ito				Kawatani & Sadeh			
Ref. No.	57/a	57/b	58/a		58/b		12/a		12/b	
Page/Fig. or Table	108/4	106/2	44/4-5		43/4-4		145/1		144/1	
	z (cm)	U (cm/s)	U (cm/s)	z (cm)	U (cm/s)	z (cm)	U (cm/s)	z (cm)	U (cm/s)	z (cm)	U (cm/s)
	15	605	450	5.08	329.2	10.16	230.0	24.0	250	24.5	220
	20	760	565	7.87	457.2	15.24	350.0	32.0	296	34.8	297
	30	923	742	10.16	512.0	20.32	425.0	49.0	394	44.4	366
	40	985	902	15.24	657.4	25.40	500.0	73.5	488	59.0	455
	45	1016	965	22.25	777.8	44.50	625.0	95.5	531	75.2	527
	50	1043	1010	25.40	823.0	62.00	675.0	103.0	572	99.7	589
	55	1062	1043	31.00	851.0			109.0	590	109.0	597

Source:	Jungle Canopy		Shinn	
Ref. No.	59		60	
Page/Fig. or Table	81/35		23/V	
	z (m)	U (cm/s)	z (m)	U (cm/s)
	32.4	282	32.6	339.0
	37.5	350	37.8	392.0
	44.1	408	44.0	428.0
	59.0	486	58.9	475.4
	182.4	900	188.5	925.0